iScience

CellPress
OPEN ACCESS

Article

Effect of diet and genotype on the lipidome of mice with altered lipoprotein metabolism

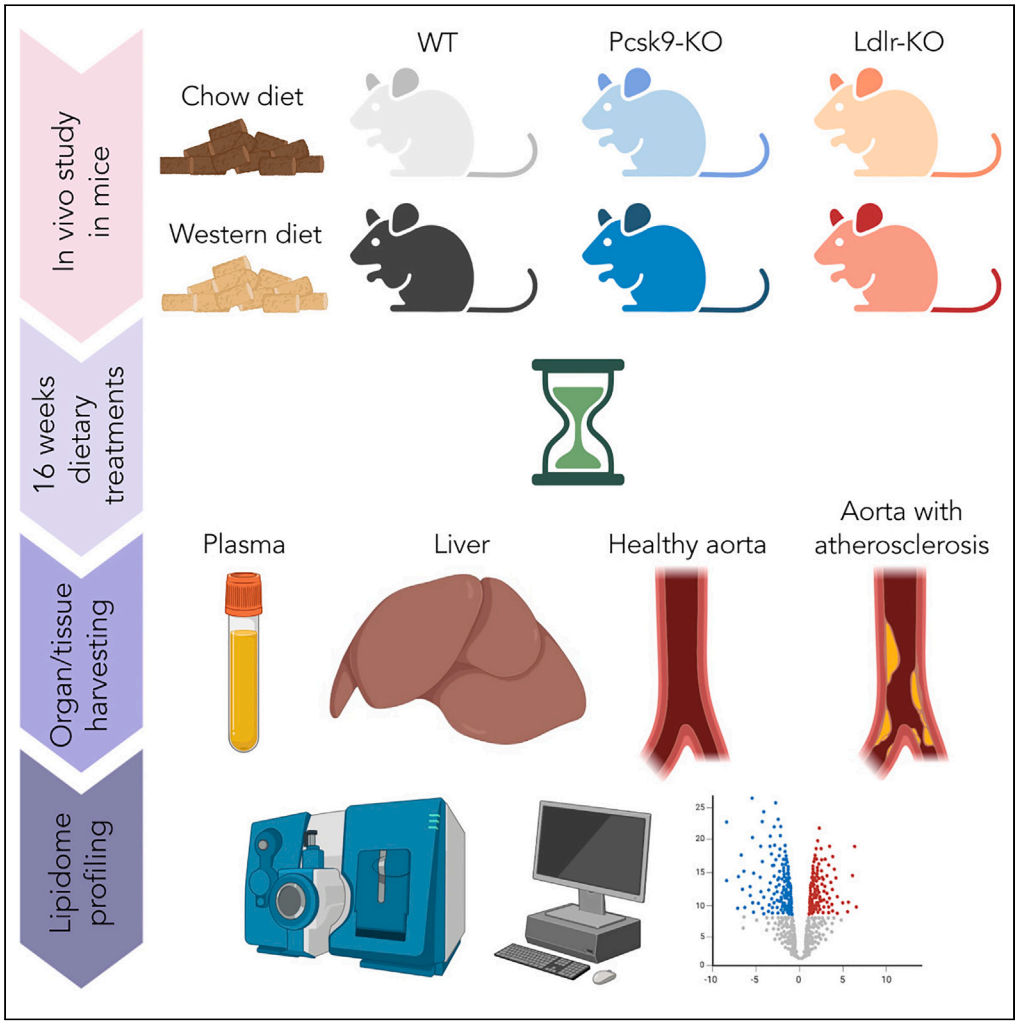

Marco Busnelli, Stefano Manzini, Alice Colombo, Elsa Franchi, Mitja Lääperi, Reijo Laaksonen, Giulia Chiesa

marco.busnelli@unimi.it (M.B.)
giulia.chiesa@unimi.it (G.C.)

Highlights

No striking differences were found between Pcsk9-KO and WT mouse lipidomes

Atherosclerotic aorta of WD-fed Ldlr-KO mice has a distinctive lipid makeup

After WD, the same16 lipids were always higher in the tissues of Ldlr-KO mice

Lipid species with matching plasma, liver, and aorta patterns may serve as biomarkers

Busnelli et al., iScience 27, 111051
October 18, 2024
https://doi.org/10.1016/j.isci.2024.111051

iScience

CellPress
OPEN ACCESS

Article

Effect of diet and genotype on the lipidome of mice with altered lipoprotein metabolism

Marco Busnelli,[1,4,5,*] Stefano Manzini,[1,4] Alice Colombo,[1] Elsa Franchi,[1] Mitja Lääperi,[2] Reijo Laaksonen,[2,3] and Giulia Chiesa[1,*]

SUMMARY

The present study describes and compares the impact of PCSK9 and LDLR, two pivotal players in cholesterol metabolism, on the whole lipidome of plasma, liver and aorta in different dietary conditions. This issue is relevant, since several lipid species, circulating at very low concentrations, have the ability to impair lipid metabolism and promote atherosclerosis development. To this aim, wild-type, hypercholesterolemic Ldlr-KO, and hypocholesterolemic Pcsk9-KO mice were fed a standard chow or a Western-type diet up to 30 and 16 weeks of age, respectively. 42 lipids including cholesterol, cholesteryl esters, several sphingolipids, phospholipids, and lysophospholipids, accumulated uniquely in the atherosclerotic aorta of Western-type diet-fed Ldlr-KO mice. In addition, multiple organ/tissue comparisons allowed us to identify 16 lipids whose plasma and hepatic patterns mirrored the lipidome of the atherosclerotic aorta. These lipid species, belonging to cholesteryl esters, glucosyl/galactosylceramide, lactosylceramide, globotriaosylceramide, sphingomyelin, and phosphatidylcholine could be further investigated as circulating biomarkers or therapeutic targets.

INTRODUCTION

Numerous studies have highlighted the significance of elevated levels of low-density lipoprotein cholesterol (LDL-C) as the primary cause of atherosclerosis.[1,2] Patients diagnosed with familial hypercholesterolemia (FH) and possessing extremely high levels of LDL-C are more prone to subclinical atherosclerosis and atherosclerosis progression, leading to a substantially increased risk of cardiovascular (CV) disease.[1,3,4] Despite statin therapy being the standard treatment for reducing lipid levels, patients with very high LDL-C rarely achieve the intended target levels.[5] Proprotein convertase subtilisin/kexin type 9 (PCSK9) inhibitors have demonstrated effectiveness in reducing LDL-C levels, preventing CV events, and regressing atherosclerotic burden.[6] They act by interfering with PCSK9, which would otherwise bind to the low-density lipoprotein receptor (LDLR) triggering its degradation. Their action leads to high levels of LDLR on the cell surface, which translates to very low LDL-C levels.

Extensive research has been conducted on the impact of PCSK9 function on LDL-C and cholesterol metabolism, but its overall impact on the whole lipidome is far less explored. Yet, there is evidence to suggest that inhibiting PCSK9 may have a significant effect on lipid metabolism. For example, a transgenic mouse model revealed that Pcsk9 deficiency affected plasma levels of several sphingolipids[7] and in patients treated with PCSK9 inhibitors, several plasma lipid classes were reduced, and sphingolipid levels were the most affected[8,9] This suggests that atherosclerosis, and thus cardiovascular risk, could be modulated by lowering lipid classes further to cholesterol in its free and esterified form.

Continuous improvements in mass spectrometry have made it possible in recent years to move rapidly from the identification of hundreds of lipid species present in atherosclerotic plaques,[10,11] to the association of different lipidomic signatures with specific features of human lesions, such as stable and unstable areas.[12]

Moreover, the evaluation of plasma lipidome is currently considered a promising strategy to better predict the atherosclerotic cardiovascular disease risk.[13–15] Ceramides represent a successful model in this regard, since the evaluation of this lipid class enabled the development of two different risk scores to be used on top of clinical characteristics. In particular, the more recent of the two, which consists of an association between four ceramides and three phospholipids, was developed and validated in three independent cohorts that included more than ten thousand patients with coronary artery disease .[16,17]

However, much effort remains to be made. From a clinical perspective, all these observations were the result of retrospective and cohort-specific studies, thus, large prospective studies are required to compare current clinical risk scores with those lipidomics-based.

[1]Department of Pharmacological and Biomolecular Sciences "Rodolfo Paoletti", Università degli Studi di Milano, via Balzaretti, 9, Milan, Italy
[2]Zora Biosciences Oy, 02150 Espoo, Finland
[3]Finnish Cardiovascular Research Center, University of Tampere, 33520 Tampere, Finland
[4]These authors contributed equally
[5]Lead contact
*Correspondence: marco.busnelli@unimi.it (M.B.), giulia.chiesa@unimi.it (G.C.)
https://doi.org/10.1016/j.isci.2024.111051

Similarly, lipidomic analyses in experimental models may provide a relevant contribution to understanding the etiopathogenesis of atherosclerosis.[18–20]

In the present study, Pcsk9 knockout and Ldlr knockout mice, as opposite models of lipoprotein metabolism and atherosclerosis susceptibility, and wild-type mice as control, were enrolled. The aim was to investigate simultaneously the lipidome of three key districts in lipid pathophysiology such as plasma, liver, and aorta. Since the composition of lipids in plasma and tissues is significantly influenced by diet,[21,22] lipidomic analysis was extended to mice fed both a standard rodent diet and a Western-type diet.

RESULTS

Body weight, liver weight, atherosclerosis development

In all the genotypes, body weight was higher in WD-fed mice compared to CD. No difference in body weight was found among groups fed CD, whereas, by comparing WD-fed mice, a lower weight of Ldlr-KO vs. WT was observed (Figure 1A). This result is in line with previous data using Western diets with a similar composition.[23,24] WD was also associated to a significantly higher liver weight compared to CD in all genotypes, with the highest weight observed in WT mice (Figure 1B). As expected, atherosclerosis development was observed only in Ldlr-KO mice either fed CD or WD. The atherosclerotic plaque area measured at the aortic sinus after 16 weeks on WD was more than forty times larger than that measured in CD-fed Ldlr-KO mice (Figures 1C and 1D).

Oil Red O staining of liver sections showed a relevant accumulation of neutral lipids in all genotypes fed WD (Figure 1E).

Global lipid patterns: Dimensionality reduction

Dimensionality reduction via PCA was applied to lipid concentrations to summarize the coarse features of individual samples within all others. In plasma, all mice clustered together, with the exception of WD-fed Ldlr-KO mice, which clustered away from the other experimental groups (Figure 1F). In the liver, all the genotypes fed CD clustered similarly. On WD, Ldlr-KO mice differentiated from WT and Pcsk9-KO (Figure 1G). In the aorta, similarly to plasma and liver, all the genotypes fed CD clustered together. On WD, Ldlr-KO mice showed a completely distinct pattern with respect to WT and Pcsk9-KO (Figure 1H).

Effect of diet on the lipidome of the three genotypes

The relative contribution of the lipid classes to the lipidome of plasma, liver, and aorta is shown in Figure S1. For all genotypes, the most abundant classes in plasma were CE, PC, FC, LPC, and TAG. Administration of WD in place of CD moderately increased the relative abundance of CE in WT (+13.6%) and Pcsk9-KO (+8.6%), whereas in Ldlr-KO, the relative increase of CE was relevant (+24.4%). In the liver of CD-fed mice, PC and FC were the main lipid classes in all genotypes. WD administration dramatically increased the relative percentage of TAG and CE, while concomitantly reducing those of PC and FC. In the aorta, TAG was the most abundant lipid class, irrespective of diet and genotype. The most remarkable difference was observed in WD-vs. CD-fed mice had a much higher relative abundance of CE occurring in Ldlr-KO mice fed WD compared to those fed CD (+1,414.3%).

The absolute concentrations of the 21 lipid classes measured in plasma, liver, and aorta of the six groups are shown in Figure 2 and a schematic representation of the pathways affected by diet is shown in Figure 3. Plasma was the district in which the dietary treatment caused the most changes in common among the three genotypes: CE, Cer d18:1, FC, Gb3, Glc/GalCer, LacCer, LPC, PC, PC O/PC P, PI, SM, TAG were always significantly increased in WD vs. CD. In the liver, 9 classes showed higher concentrations in WD compared to CD in all genotypes (CE, DAG, FC, Gb3, LacCer, LPI, PA, PG, TAG). In the aorta, significant variations common to WT, Pcsk9-KO, and Ldlr-KO were limited to PE and PG, which were higher in WD vs. CD.

Changes in individual lipid concentrations in plasma, liver, and aorta of mice fed CD vs. WD are shown in Figures S2–S4, respectively. The largest quantitative changes in plasma were observed in Ldlr-KO mice, where several CE and TAG species were the ones mostly increased by WD. No striking differences among genotypes were observed in the concentration changes of lipids in the liver and aorta, except for a major accumulation of CE species in the aorta of Ldlr-KO mice fed WD.

Consistent with the different content of fatty acids 18:1 and 18:2 between CD and WD (Table 1), the lipid species containing the fatty acid 18:1 were more concentrated in plasma, liver and aorta of all WD-fed mice, whereas the species containing the fatty acid 18:2 and 20:4 - being 18:2 the precursor of the endogenous synthesis of the fatty acid 20:4 - showed reduced or unaltered concentrations in plasma, liver and aorta of WD-vs. CD-fed mice (Figures S2–S4). With the inclusion of, but not limited to, 18:1- and 18:2-containing species, a narrow panel of 28 lipids was found always increased (two CEs, one dihydroceramide, two TAGs, two LPC, three PC), or decreased/unchanged (all phospholipids; two PC, several PE or PE O/PE P and PS), in plasma, liver, and aorta of all genotypes (Figure 4).

Effect of proprotein convertase subtilisin/kexin type 9 deletion on the lipidome of plasma, liver, and aorta

The most pronounced differences between the lipidomes of WT and Pcsk9-KO mice were found in plasma, where several lipid classes were significantly less abundant in Pcsk9-KO mice, both on CD and WD (Figures 2A and 5).

In the liver, the lipidome of the two genotypes was substantially indistinguishable, and only two classes differed after WD feeding: CE, which was less abundant, and Cer d18:1, which was more abundant in Pcsk9-KO mice (Figures 2B and 5).

In the aorta, where both genotypes do not develop atherosclerosis, the major differences were evident on CD: only CE was significantly less abundant in Pcsk9-KO mice, whereas the concentrations of PA and several sphingolipid classes (Cer d18:0, Glc/GalCer, Gb3) were higher

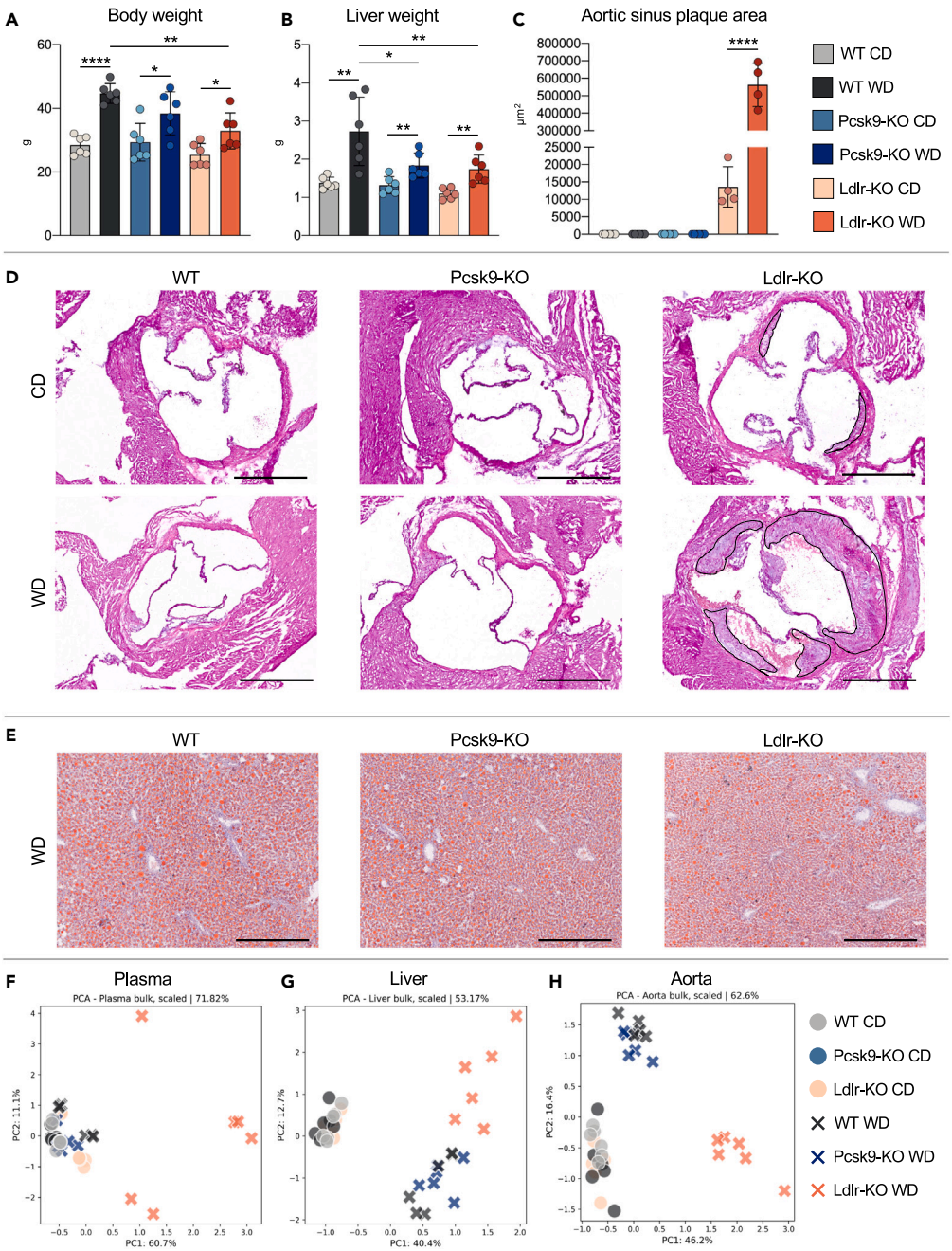

Figure 1. Effect of dietary treatment on mouse phenotype and global lipid pattern

Body weight (A) and liver weight (B) at the end of the dietary treatments are shown. Histological measurement of atherosclerosis development (C) and representative hematoxylin and eosin staining of atherosclerotic plaques in the aortic sinus of mice fed CD and WD (D) are also shown, together with representative images of Oil Red O staining of WD-fed mouse livers (E). Scatterplots of the first two principal components (PCs) are shown for each sample, calculated from each analyte concentration in plasma (F), liver (G), and aorta (H). Bar length = 500 µm. Data are shown as mean ± SD. *$p < 0.05$, **$p < 0.01$, ***$p < 0.001$, ****$p < 0.0001$. Significant differences within the same genotype (diet comparison) were determined by T-test, whereas differences among groups fed the same diet (genotype comparison) were determined by ANOVA followed by Tukey's post-hoc test. n = 4–6 per group.

in Pcsk9-KO. On WD, the differences between the two genotypes were few, and only PG and TAG were lower in Pcsk9-KO mice (Figures 2C and 5).

Analysis of the individual species (Figures S5–S10) showed that between WT and Pcsk9-KO there were no lipids varying independently of diet in the liver and aorta. In contrast, in plasma, 32 lipids were significantly less abundant in Pcsk9-KO with both dietary treatments (Figure 6).

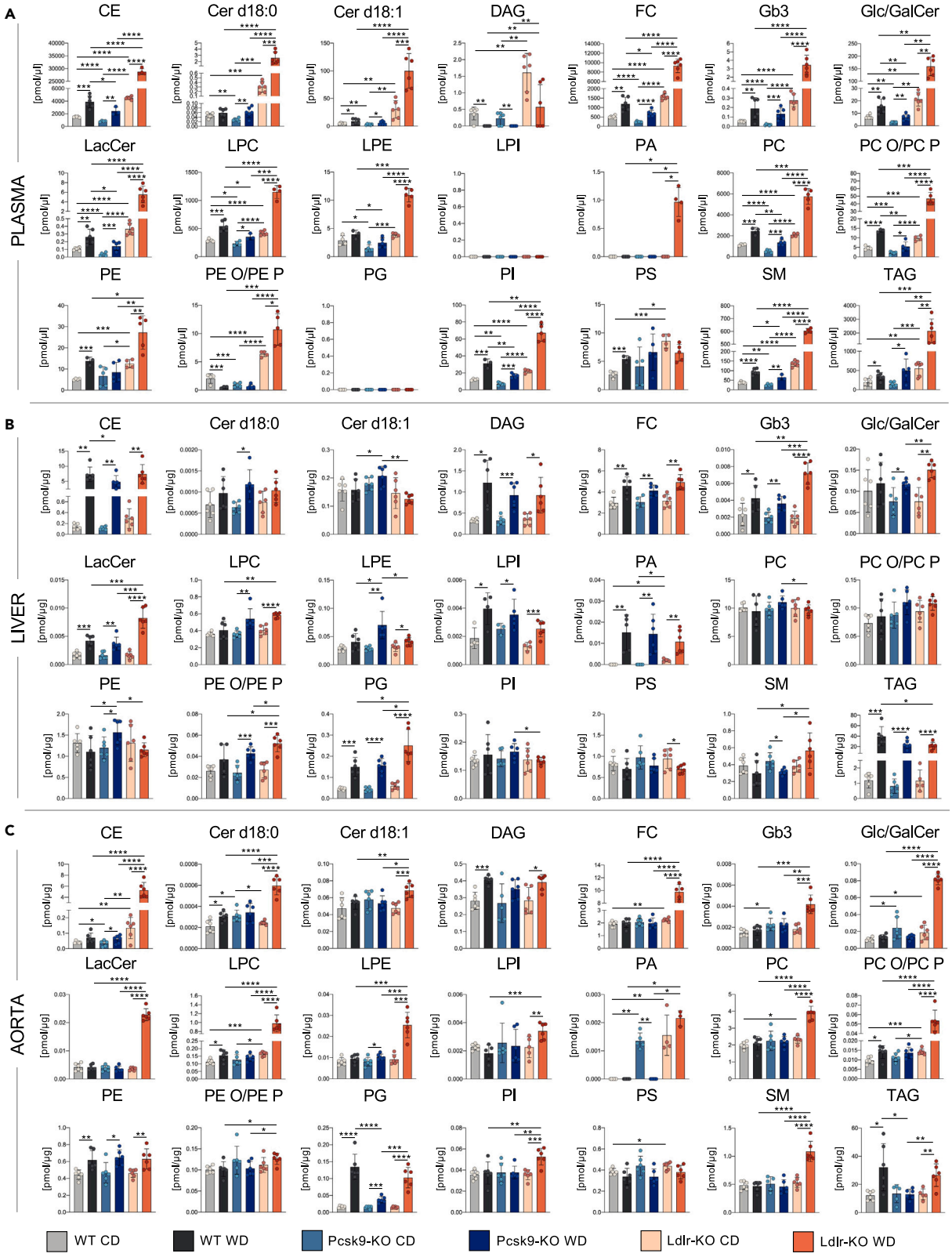
A
PLASMA
CE
Cer d18:0
Cer d18:1
DAG
FC
Gb3
Glc/GalCer
LacCer
LPC
LPE
LPI
PA
PC
PC O/PC P
PE
PE O/PE P
PG
PI
PS
SM
TAG
B
LIVER
C
AORTA
[pmol/µl]
[pmol/µg]
WT CD
WT WD
Pcsk9-KO CD
Pcsk9-KO WD
Ldlr-KO CD
Ldlr-KO WD

Figure 2. Lipid class concentrations in the three districts analyzed

Concentration of lipid classes in plasma (A), liver (B), and aorta (C) are shown as mean ± SD. *$p < 0.05$, **$p < 0.01$, ***$p < 0.001$, ****$p < 0.0001$. Significant differences within the same genotype (diet comparison) were determined by T-test, whereas differences among groups fed the same diet (genotype comparison) were determined by ANOVA followed by Tukey's post-hoc test. n = 4–6 per group.

Effect of low-density lipoprotein receptor deletion on the lipidome of plasma, liver, and aorta

Ldlr deficiency, predisposing to severe hyperlipidemia, primarily impacted on plasma. In this district, Ldlr-KO mice had increased plasma concentrations of almost all classes analyzed compared with the other two genotypes after both dietary treatments (CE, Cer d18:0, Cer d18:1, DAG, FC, Gb3, Glc/GalCer, LacCer, LPC, PC, PC O/PC P, PE, PE O/PE P, PI, PS, SM, TAG) (Figures 2A and 7). In line with what was observed for the classes, on both diets, most of the lipid species were significantly more concentrated in Ldlr-KO than in the other two genotypes. Under no case, a single lipid species was found significantly more abundant in WT or Pcsk9-KO than in Ldlr-KO mice (Figures S5 and S6).

In liver, on the other hand, the impact due to the lack of Ldl receptor was very small: on CD only the PA class was significantly increased compared with the other two genotypes. On WD, two classes of phospholipids (PE O/PE P and PG) and three classes of sphingolipids (Gb3, LacCer, and SM) were increased in Ldlr-KO mice (Figures 2B and 7). Coherently with this observation, on CD only a few species belonging to CE, LPC, PC, PE, and TAG were more concentrated in Ldlr-KO than in WT and Pcsk9-KO (Figure S7). On WD, several species belonging to Gb3, LacCer, and SM had significantly increased concentrations in Ldlr-KO (Figure S8). Although CE class concentration was not different among genotypes (Figure 2B), several CE species were more abundant in Ldlr-KO mice (Figure S8). Interestingly, only two lipid species were less abundant in the liver of Ldlr-KO mice compared with WT and Pcsk9-KO: Cer(d18:0/20:0) and Cer(d18:1/20:0) (Figure S8).

In the aorta, the differences between Ldlr-KO and the other two genotypes on CD were limited to CE, LPC, and PC O/PC P (Figures 2C and 7). Looking at individual lipids, there was a very limited number of species that were more abundant in the aorta of Ldlr-KO mice than in the other two genotypes, including all measured CE (16:0, 16:1, 18:1, 18:2, 20:4, 20:5, 22:6), several LPC (18:0, 18:2, 22:6) and one SM (d18:1/15:0) (d18:1/14:1-OH) (Figure S9). No species belonging to LacCer, PG, PI, PS, or TAG differed between the two athero-resistant genotypes and Ldlr-KO mice (Figure S9).

On WD, atherosclerotic lesions developed only in the aorta of Ldlr-KO mice. Coherently, differences between the pro-atherogenic genotype and the other two genotypes increased dramatically and as many as 15 lipid classes were more concentrated in Ldlr-KO mice (Figures 2C and 7). The sterol pathway (CE, FC), the whole sphingolipid pathway (Cer d18:0, Cer d18:1, LacCer, Glc/GalCer, Gb3, SM), and much of the phospholipid pathway (LPC, LPE, PA, PC, PC O/PC P, PE O/PE P, PI) were upregulated. Conversely, glycerolipids (DAG and TAG) were unmodified (Figure 7). In terms of lipid species, CE was present in markedly increased amounts, particularly the species containing 16:0, 18:1, 20:3, and 22:6 residues (Figures 8 and S10). Other species whose concentration was particularly high in Ldlr-KO

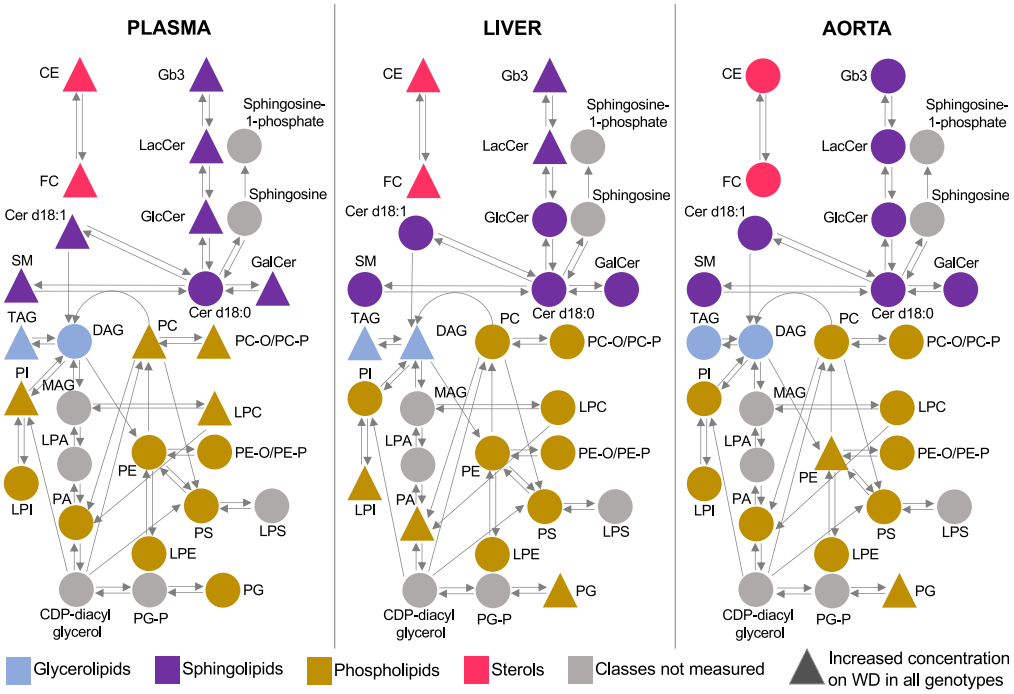

Figure 3. Overall effect of the Western diet on the lipid pathways analyzed

The pathways involving the lipid classes measured in plasma, liver, and aorta of the three genotypes are represented. Triangles identify those lipid classes whose concentration was increased by WD in all genotypes.

Table 1. Mean percentage of the fatty acid content of the two diets (% w/w)

Fatty acid	Chow (4RF21)	Western (TD.88137)
C4:0	ND	0.435
C6:0	ND	0.311
C8:0	ND	0.228
C10:0	ND	0.538
C12:0	0.006	0.683
C14:0	0.030	2.194
C16:0	0.383	5.982
C16:1	0.024	0.311
C18:0	0.084	2.588
C18:1 oleic	0.511	4.326
C18:1 isomers	ND	0.828
C18:2 linoleic	1.298	0.476
C18:2 isomers	ND	0.269
C18:3 linolenic	0.247	0.145

mice were: FC, Glc/GalCer(d18:1/16:0), Glc/GalCer(d18:1/22:0) Glc/GalCer(d18:1/22:1) Glc/GalCer(d18:1/23:0) Glc/GalCer(d18:1/24:0) Glc/GalCer(d18:1/24:1) Glc/GalCer(d18:1/26:0), Glc/GalCer(d18:1/26:1), LacCer(d18:1/16:0), LacCer(d18:1/22:0), LacCer(d18:1/23:0), LacCer(d18:1/24:0), LacCer(d18:1/24:1), LPC 16:0, LPC 16:1, LPC 18:0, LPC 18:1, LPC 18:2, LPC 20:3, SM (d18:1/15:0) (d18:1/14:1-OH) (Figures 8 and S10). It is noteworthy to observe that Cer(d18:1/20:0) was the only less abundant lipid in the aorta of Ldlr-KO mice than in WT and

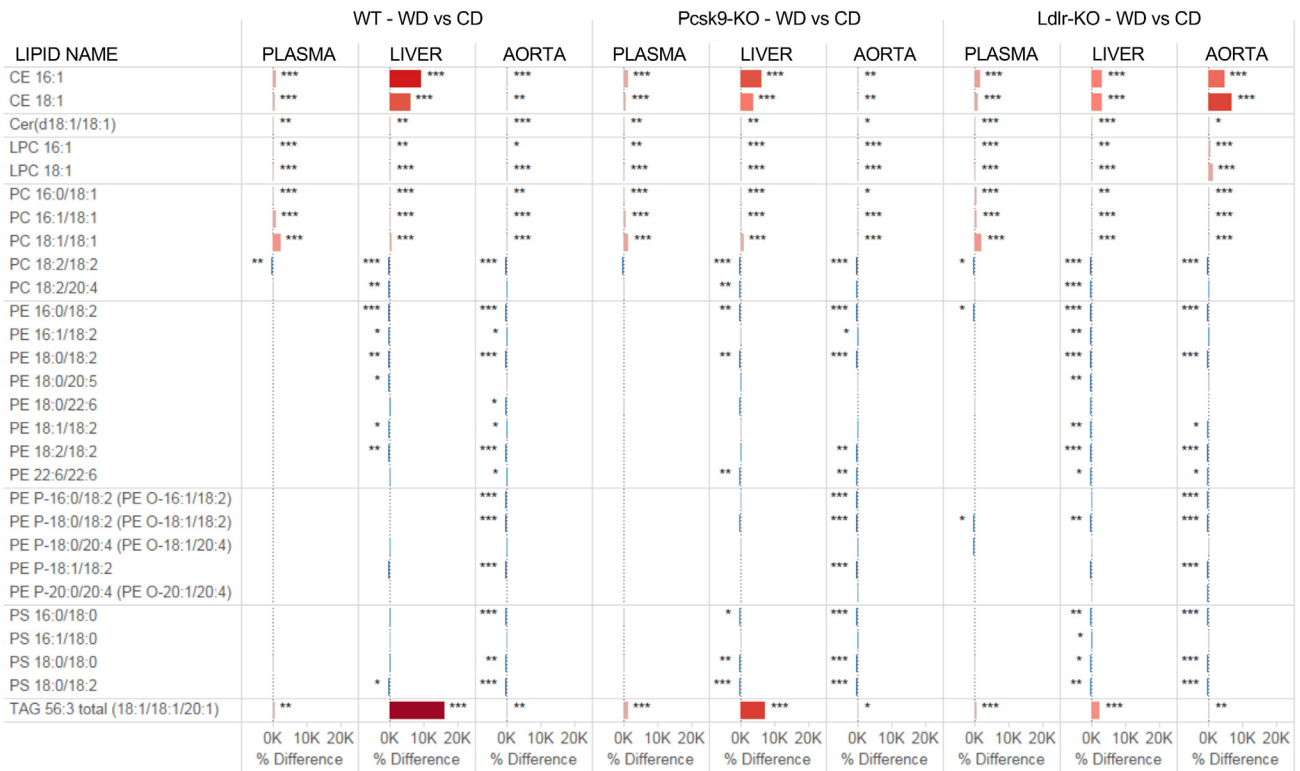

Figure 4. Median changes of the 28 lipid species whose concentration is increased or decreased/unchanged by Western diet in all districts and genotypes

Lipid species increased by WD vs. CD in plasma, liver and aorta of WT, Pcsk9-KO, and Ldlr-KO mice are shown with red bars, whereas those decreased by WD are shown with blue bars. Significant differences were determined by T test. *$p < 0.05$; **$p < 0.01$, ***$p < 0.001$. n = 3–6 per group.

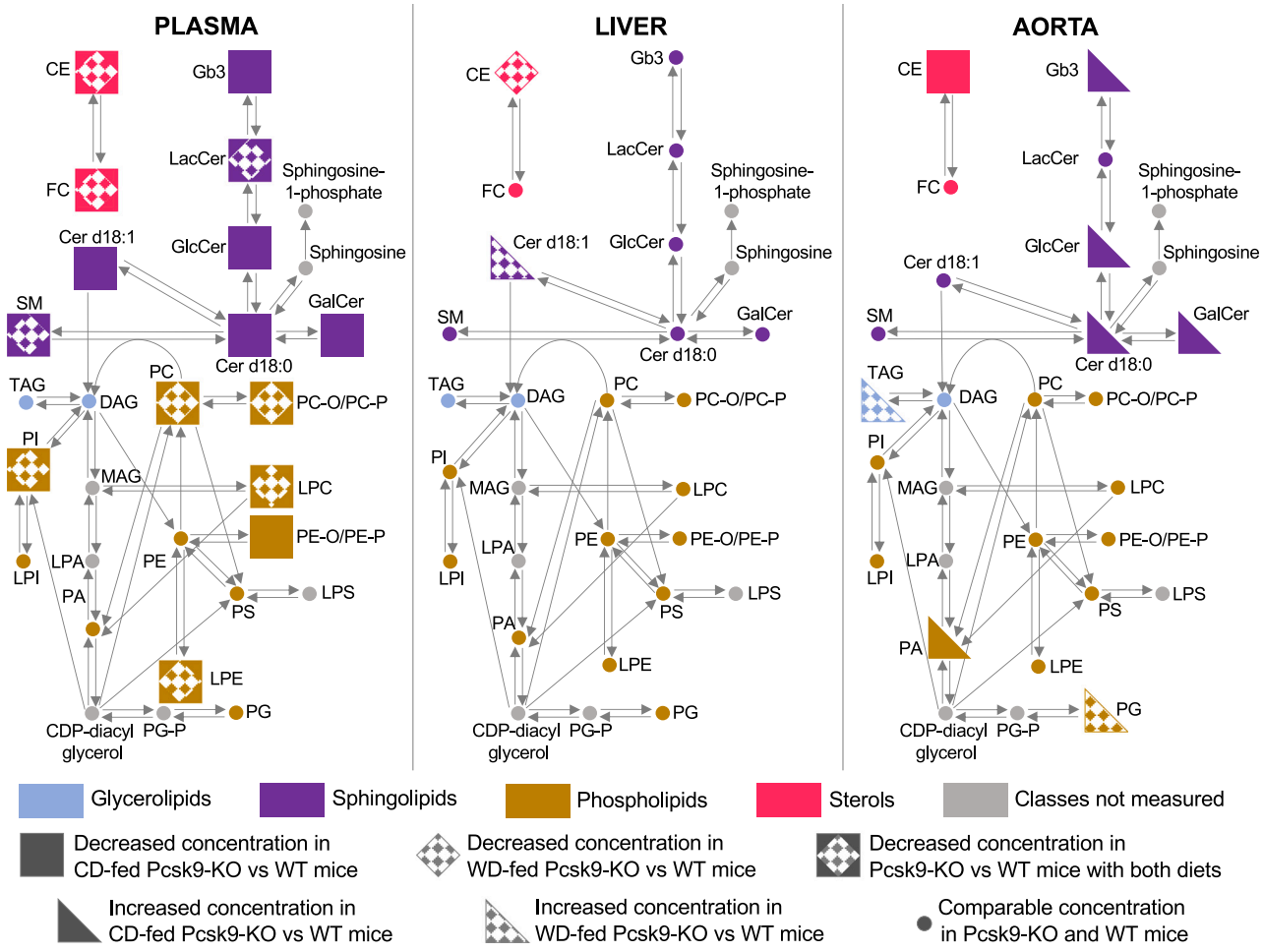

Figure 5. Overall effect of Pcsk9 deletion on the lipid pathways analyzed

The pathways involving the lipid classes measured in plasma, liver, and aorta of Pcsk9-KO and WT mice are represented. Squares/diamonds identify decreases and triangles identify increases in those lipid classes whose concentration was significantly different between Pcsk9-KO and WT mice. Filled symbols refer to differences between CD-fed mice, chequered symbols highlight differences between WD-fed mice.

Pcsk9-KO mice. Additionally, there were 78 lipid species whose amount did not vary across athero-prone and athero-resistant genotypes (Figure S10).

Some lipids never showed increased concentration in the presence of aortic atherosclerosis, either when Ldlr-KO were compared with the other two genotypes or when the two dietary treatments were compared in Ldlr-KO: PE 18:0/20:5, PS 16:1/18:0, SM(d18:0/17:0)(d18:1/16:0-OH), PI 18:1/18:1, DAG 16:1/18:0, PS 18:0/22:5, Cer(d18:0/18:0), Cer(d18:1/20:0), Cer(d18:1/18:0) (Figures S4 and S10).

Overall observations

To evaluate if each genotype was characterized by a peculiar lipid pattern that emerged independently from the dietary treatment, lipidome variations among WT, Pcsk9-KO, and Ldlr-KO mice fed both CD and WD were compared.

Comparison among the lipidomes of CD-fed mice showed that the same three lipids (CE18:2, CE20:4, CE22:6) were increased in Ldlr-KO plasma, aorta and liver vs. both WT and Pcsk9-KO mice (Figures S5, S7, S9, and S11). On WD, among all lipid species measured in the three organs/tissues, only 16 were always significantly more concentrated in Ldlr-KO than in the other two genotypes: CE 18:2, CE 20:3, CE 22:6, Gb3(d18:1/22:0), Gb3(d18:1/24:0), Gb3(d18:1/24:1), Glc/GalCer(d18:1/16:0), LacCer(d18:1/16:0), LacCer(d18:1/22:0), LacCer(d18:1/24:0), LacCer(d18:1/24:1), PC 16:0/16:0, PC P-18:0/20:4 (PC O-18:1/20:4), SM(d18:1/15:0) (d18:1/14:1-OH), SM(d18:1/16:0) (d18:1/15:1-OH), SM(d18:1/16:1) (d18:1/15:2-OH) (Figure 9). Moreover, as described above, Cer(d18:1/20:0) was the only species to be significantly less abundant in the aorta and liver of Ldlr-KO mice compared with WT and Pcsk9-KO mice (Figures S8, S10, and S11).

By cross-referencing the lipid profiles obtained from the comparison of the dietary treatments in Ldlr-KO mice with those obtained from the comparison of WD-fed Ldlr-KO mice with the other two genotypes, it was possible to identify 42 species whose aortic concentration was always increased in WD-fed Ldlr-KO mice, i.e., in the presence of atherosclerotic plaques (Figure 10).

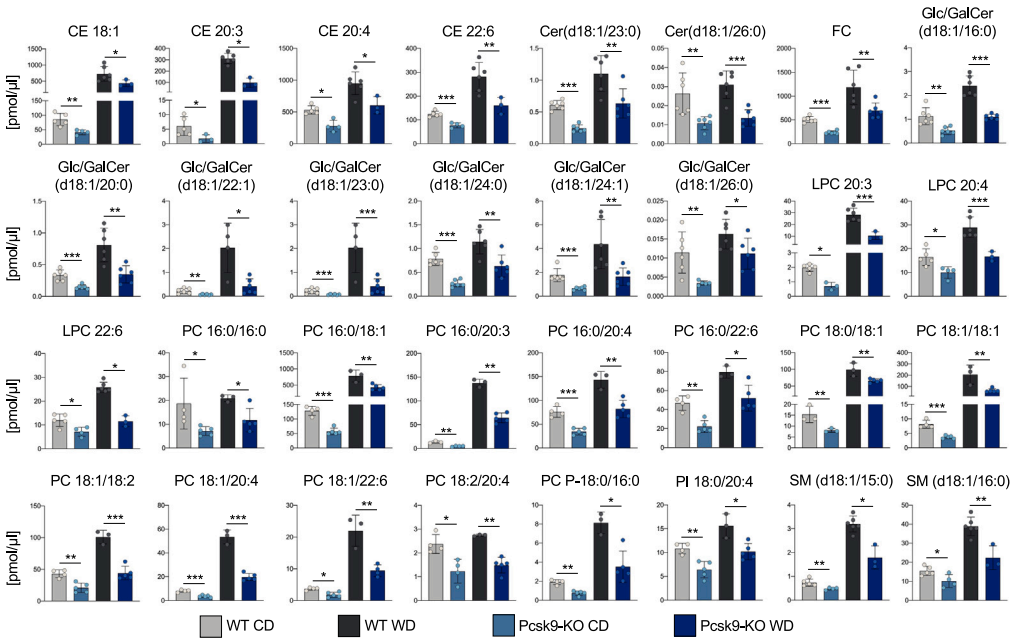

Figure 6. Plasma levels of the 32 lipid species whose concentration was lower in Pcsk9-KO vs. WT mice with both dietary treatments

Significant differences were determined by T test. *$p < 0.05$; **$p < 0.01$, ***$p < 0.001$. n = 3–6 per group.

DISCUSSION

It is well known that, in humans, loss-of-function mutations in the LDLR gene determine familial hypercholesterolemia,[25] whereas loss-of-function mutations in the PCSK9 gene are associated with hypocholesterolemia and reduced risk of developing coronary heart disease.[26]

The aim of this work was to move beside cholesterol levels and analyze how the whole lipidome varied in plasma, liver, and aorta obtained from WT mice, as well as mice constitutively lacking PCSK9 or LDLR. In order to achieve a more informative characterization, mice were fed a standard chow diet (CD) or a Western diet (WD).

These two diets differ in the amount of fat and the relative abundance of different fatty acids. Most importantly, they differ in the amount of cholesterol: only trace amounts are present in the chow diet, and about 100 times more are in the Western diet.

The comparison in terms of class concentrations indicated that plasma was the main district to be affected by dietary changes in all genotypes. Coherently to its relevant role in lipid metabolism, also the liver showed several increases in lipid class concentrations in all WD-fed groups, whereas in the aorta, only two classes of phospholipids were affected by diet in a genotype-independent manner. Looking at individual lipids, species belonging to most lipid classes increased after the administration of the WD, with those belonging to CE showing the greatest increase in plasma of all genotypes and, limited to Ldlr-KO mice, in the aorta. In the liver, in addition to CE, several TAG analytes increased dramatically following WD administration in a genotype-independent manner. Indeed, fatty liver disease was detected in all groups fed WD.

The different fatty acid compositions of the two diets impacted the concentration of these residues in several lipid classes of all the districts analyzed. Specifically, the dietary concentration of the essential fatty acid 18:2 (0.476% w/w in WD vs. 1.298% w/w in CD) may explain why plasma, liver, and aorta of mice fed WD showed low levels of lipid species carrying this fatty acid as residue. Further, being the fatty acid 18:2 the precursor in the endogenous synthesis of fatty acid 20:4, most lipids containing 20:4 residue were also at lower concentration in WD-fed mice compared with CD-fed mice. The difference in the 18:1 content of the two diets also explained the higher concentrations of 18:1-containing species in WD fed mice, in all districts.

The extremely high content of palmitic acid in WD significantly increased the concentration of lipids containing fatty acid 16:0 mostly in plasma and liver. Saturated fatty acids are known to exert pro-inflammatory effects on many leukocyte subsets of the innate and adaptive immunity,[27,28] and macrophages exposed to fatty acid 16:0 have been shown to increase their secretion of several cytokines/chemokines as well as neutrophil-attracting nucleotides.[29,30] Likewise, excess cholesterol may promote the activation and migration into tissues of proinflammatory innate and adaptive immune cells. Cholesterol accumulation in plasma membranes of neutrophils and macrophages results in increased toll-like receptor signaling and NLRP3 inflammasome priming.[31,32] Additionally, plasma membrane cholesterol increases T cell receptor signaling in in $CD8^+$ T-cells, thus increasing lymphocyte proliferation.[33] All these observations are extremely relevant in view of the established role of inflammation in both fatty liver disease and atherosclerosis.

A focus of this work was the evaluation of a possible lipidome modification in the presence or absence of PCSK9. In plasma, the lack of Pcsk9 deeply influenced lipid class composition after both dietary treatments and these changes affected sterols, phospholipids and sphingolipids. Surprisingly, these perturbations in circulating lipids were not paralleled by comparable changes in the liver: no variations were observed between WT and Pcsk9-KO on CD, and only two classes varied on WD.

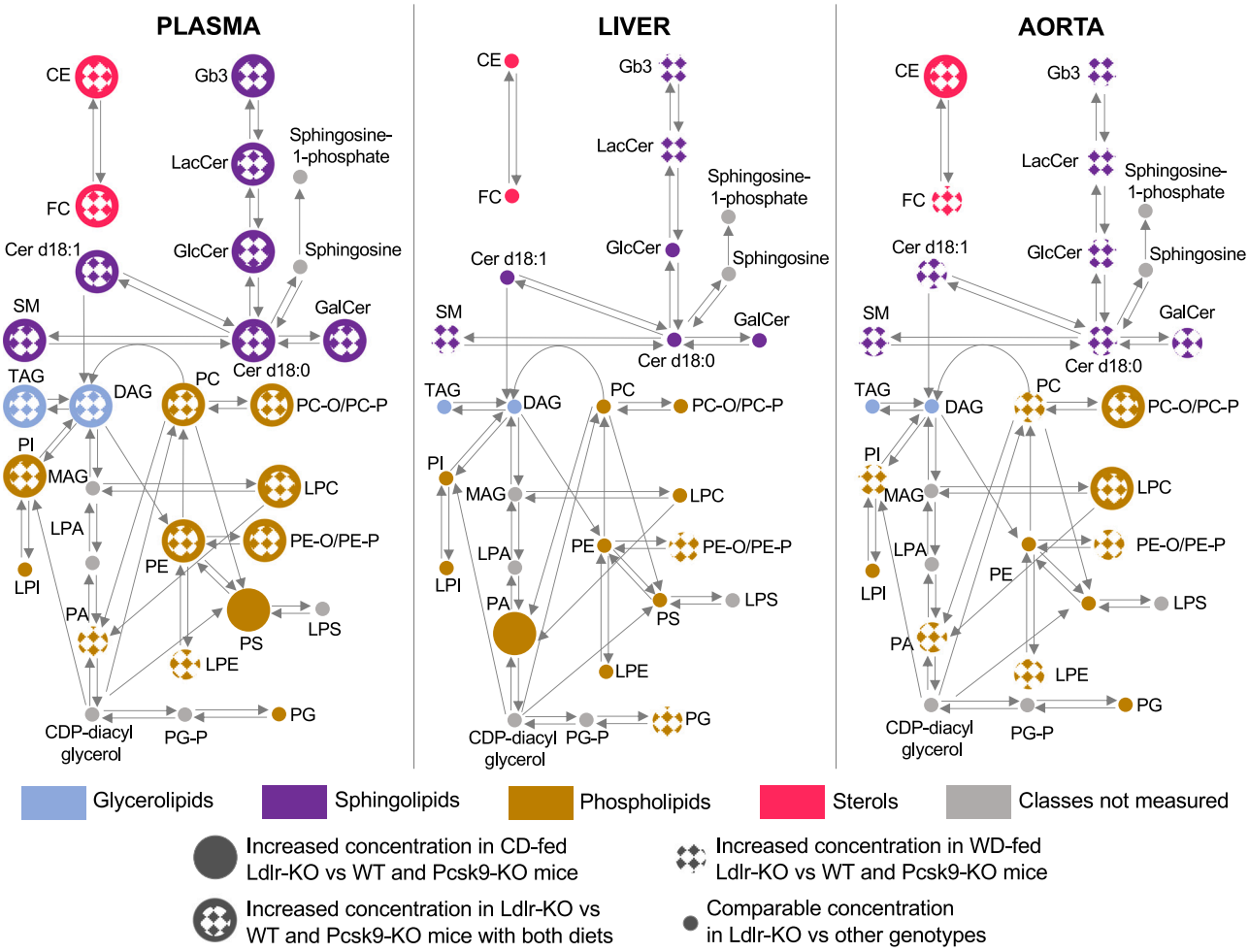

Figure 7. Overall effect of Ldlr deletion on the lipid pathways analyzed

The pathways involving the lipid classes measured in plasma, liver, and aorta of Ldlr-KO, Pcsk9-KO, and WT mice are represented. Larger circles identify those lipid classes whose concentration was significantly increased in Ldlr-KO mice vs. WT and Pcsk9-KO mice. Filled circles refer to differences among CD-fed mice, chequered circles highlight differences among WD-fed mice.

The lipid species that were less abundant in the plasma of Pcsk9-KO vs. WT after both diets belonged to CE, FC, sphingomyelins (Cer d18:1, Glc/GalCer, LacCer, SM), and phospholipids. A previous study already showed a reduction in plasma lipids belonging to these classes in liver-specific Pcsk9 knockout mice compared with WT mice when fed a standard rodent diet, without investigating the effect determined by Western diet administration.[7] Our result is also remarkably in line with that obtained in a study comparing the plasma lipidome obtained from patients receiving anti-Pcsk9 therapy or placebo for 29 days. In that investigation, the inhibition of Pcsk9, besides plasma levels of LDL-C and non-HDL-cholesterol, markedly reduced sphingolipids (Cer d18:0, Cer d18:1, Gb3, Glc/GalCer, LacCer, SM), CE and FC, and to a lesser extent phospholipids.[9] Is it interesting to note that the absence of Pcsk9 did not lead to a specific lipid signature in the liver and aorta, since no relevant differences between Pcsk9-KO and WT mice were consistently observed with both dietary treatments.

A second focus of this work was the evaluation of the impact of the LDL receptor deficiency on the whole lipidome, additional to the well-known hypercholesterolemic condition.

In the plasma of Ldlr-KO, the concentration of almost all lipid classes was higher than in the other two genotypes on both dietary treatments. Also in these comparisons, the liver was much less susceptible to genotype-related lipidome variations than plasma.

In the aorta, as expected, a relevant increase of several lipid classes and species was observed only in Ldlr-KO fed WD where atherosclerotic plaques developed compared with the two athero-resistant genotypes. The analysis was performed on the entire aorta and not only on atherosclerotic plaques, so it is not surprising that the most abundant lipid class was TAG, which, by contrast, does not contribute to plaque burden.[34] Specifically, no differences in TAG species were observed between WT and Ldlr-KO, whereas Pcsk9-KO showed a different profile, in which several aortic TAG species were significantly less concentrated than in both Ldlr-KO and WT.

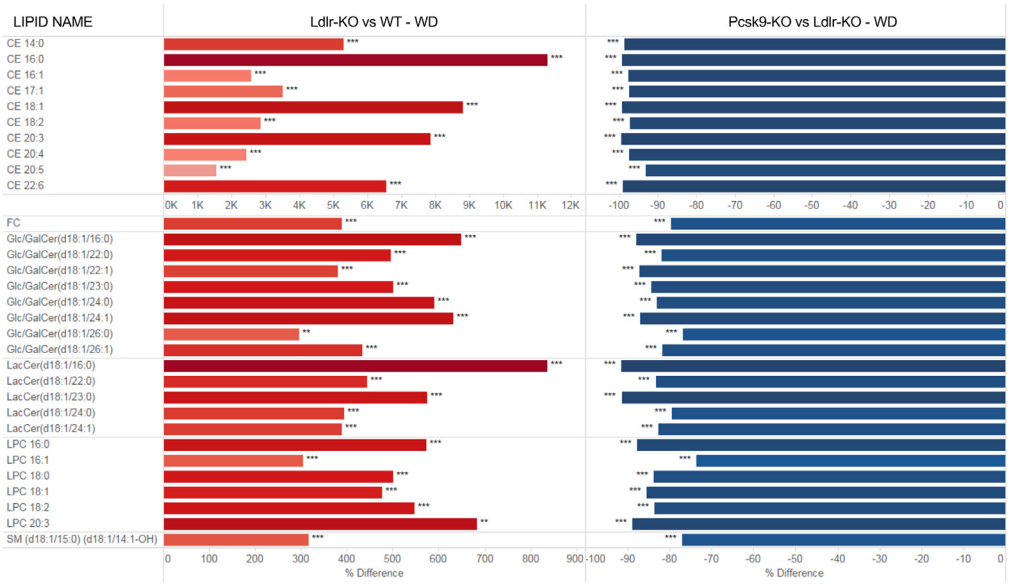

Figure 8. Median changes of the lipid species showing the highest increase in the aorta of Ldlr-KO mice vs. both WT and Pcsk9-KO mice on WD feeding

Red bars indicate that the concentration is increased in the first comparison term, blue bars indicate that the concentration is reduced in the first comparison term. Significant differences were determined by T test. *$p < 0.05$; **$p < 0.01$, ***$p < 0.001$. n = 3–6 per group. See also Figure S10.

A number of lipid species belonging mainly to DAG, PE, and PE O/PE P did not differ between Ldlr-KO and the other two genotypes. These species could belong to classes that do not accumulate in the plaque or whose concentrations are finely regulated as fundamental elements in the homeostasis of the arterial wall.

In contrast, only in the presence of atherosclerotic plaques, the whole aorta lipidome showed increased concentrations of 42 lipid species. Such lipids might indeed represent markers that accumulate in the arterial wall only in the presence of established lesions.

A handful of CE together with FC were abundant in plaques: it is well known that LDL that aggregate in the subendothelial space contain a core rich in CE that undergoes extracellular hydrolysis and this leads to the accumulation of abundant FC in atherosclerotic plaques.[35]

A large number of sphingolipids (25 out of 42 lipid species) showed significantly increased concentrations in the presence of atherosclerotic lesions; these included Cer d18:0, Cer d18:1, LacCer, Glc/GalCer, Gb3, and SM. These increases were so marked that even at the level of lipid classes, sphingolipids were more abundant in the diseased aorta than in the healthy aorta. Several studies have demonstrated the importance of sphingolipids, and particularly ceramides, in inflammatory-related diseases, such as atherosclerosis.[36] Indeed, an increased concentration of ceramide modulates toll-like receptor stimulation of macrophages, whereas, in neutrophils, it mediates cell migration, generation of reactive oxygen species, and neutrophil extracellular trap formation.[37,38] Moreover, ceramides are also involved in the fine-tuning of T lymphocyte responses.[39]

According to our findings, it has been previously demonstrated that LDL within atherosclerotic lesions is particularly enriched in ceramides.[40] Thus, plasma ceramides have been investigated as potential markers of cardiovascular disease, and the ratios between specific plasma ceramides [Cer(d18:1/16:0)/Cer(d18:1:/24:0), Cer(d18:1/18:0)/Cer(d18:1:/24:0), Cer(d18:1/24:1)/Cer(d18:1:/24:0)] have been proposed as predictive for fatal cardiovascular events above currently used lipid markers.[41] In our study, only the Cer(d18:1/24:1)/Cer(d18:1:/24:0) ratio was significantly increased in plasma of Ldlr-KO fed WD compared with both Ldlr-KO fed CD ($p = 0.0000003671$, data not shown) and WT mice fed WD ($p = 0.0000108608$, data not shown), but not with Pcsk9-KO ($p = 0.217$, data not shown).

Sphingomyelins were the first class of sphingolipids to be identified in atherosclerotic plaques.[42] Beyond sphingomyelins, the presence of ceramides, lactosylceramides, and glucosylceramides was subsequently identified as a common sphingolipid signature of carotid plaques.[43,44] In addition, although globotriaosylceramides have never been directly implicated in atherosclerosis, it has been observed that their excessive accumulation in the lysosomes of Fabry Disease subjects promotes endothelial dysfunction.[45,46] Therefore, their contribution to atherosclerosis development cannot be excluded and indeed requires further investigation.

Several phospholipids and lysophospholipids were particularly abundant in the presence of arterial lesions. Several lysophospholipid species have been recently identified as atheroma-specific lipids in plaques developing in the aortic root of athero-prone mice, including Ldlr-KO mice.[20] In particular, LPCs have been recognized as relevant signaling molecules produced under physiological conditions by the action of phospholipase A2 on phosphatidylcholine.[47] LPC species have been associated with the high-risk plaque phenotype[48] and are particularly abundant on oxidized LDL that accumulates in the subendothelial space.[49] Since LPC has an activating effect on a wide range of immune cells,[50–54] many proinflammatory effects of oxidized LDL are thought to depend on bioactive LPC.[47]

These 42 species could therefore represent markers or molecular targets to be addressed, dietetically or pharmacologically. To give further relevance to these potential markers, their levels were assessed in lipidomics previously performed by our group in apoE-KO

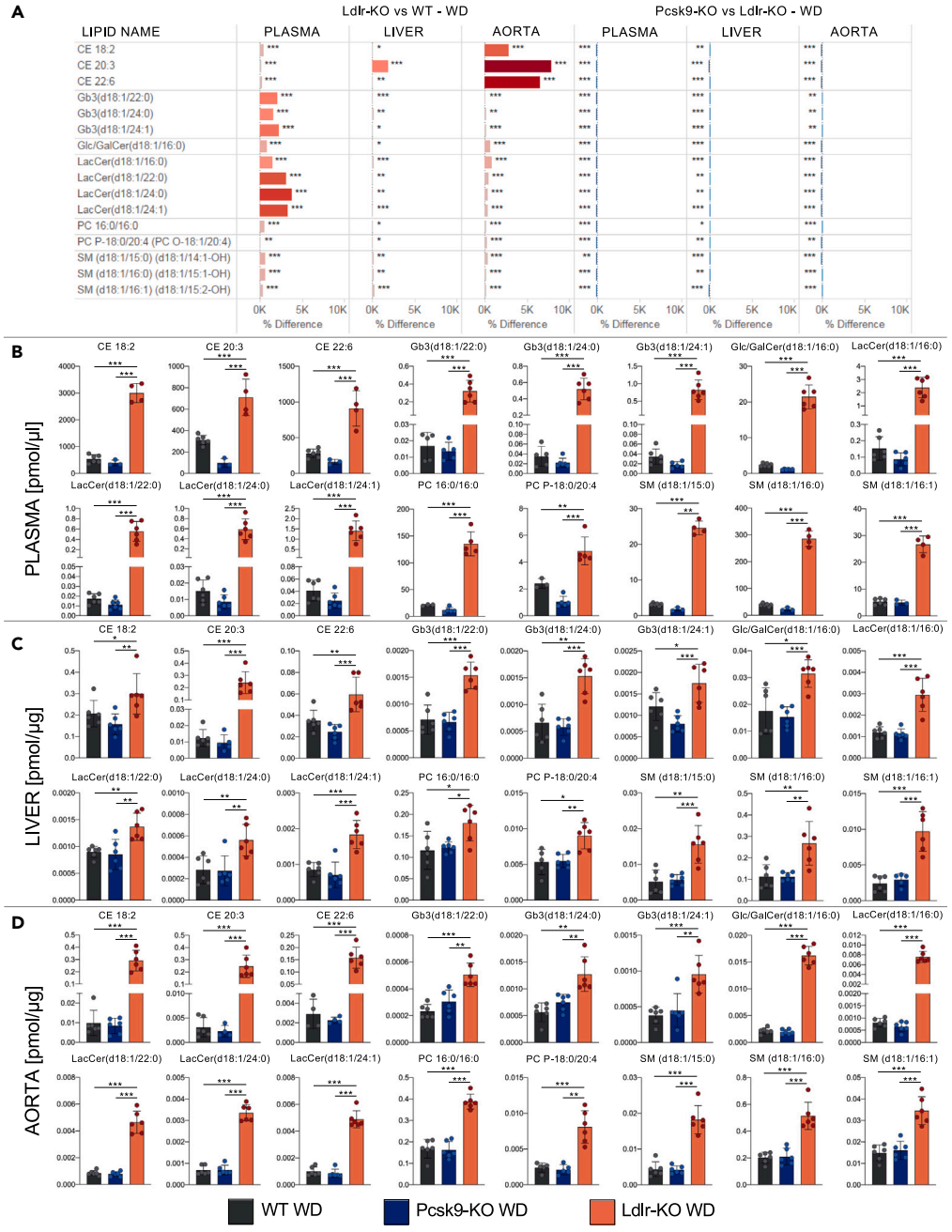

Figure 9. Lipid species increased in plasma, liver, and aorta of WD-fed Ldlr-KO mice compared with WT and Pcsk9-KO mice

Median changes (A) and absolute concentrations in plasma (B), liver (C) and aorta (D) are shown. Sixteen lipid species emerged from this analysis. Red bars indicate that the concentration is increased in the first comparison term, and blue bars indicate that the concentration is reduced in the first comparison term. Significant differences were determined by T test. *$p < 0.05$; **$p < 0.01$, ***$p < 0.001$. n = 4–6 per group.

mice.[21] Although all the same lipid species were not available, also in this pro-atherogenic model it was possible to confirm that most of these lipids had increased concentration in aortic segments with large atherosclerotic plaques (Figures S12A and S12B).

However, atherosclerotic plaques develop over decades in several arterial districts. Often, the detection of plaques occurs when cardiovascular/cerebrovascular symptoms are already underway such that emergency interventions are required. Therefore, even more relevant would be the identification of lipids in circulation or other body districts that serve as reliable and readily quantifiable markers for better profiling/stratification of patients. To this aim, in this work, 16 lipid species were identified that, in addition to being most prevalent in atherosclerotic plaque, were concurrently increased in circulating plasma and liver (Figure 9). Among them, CE 18:2 is enriched in both the plasma and liver of patients

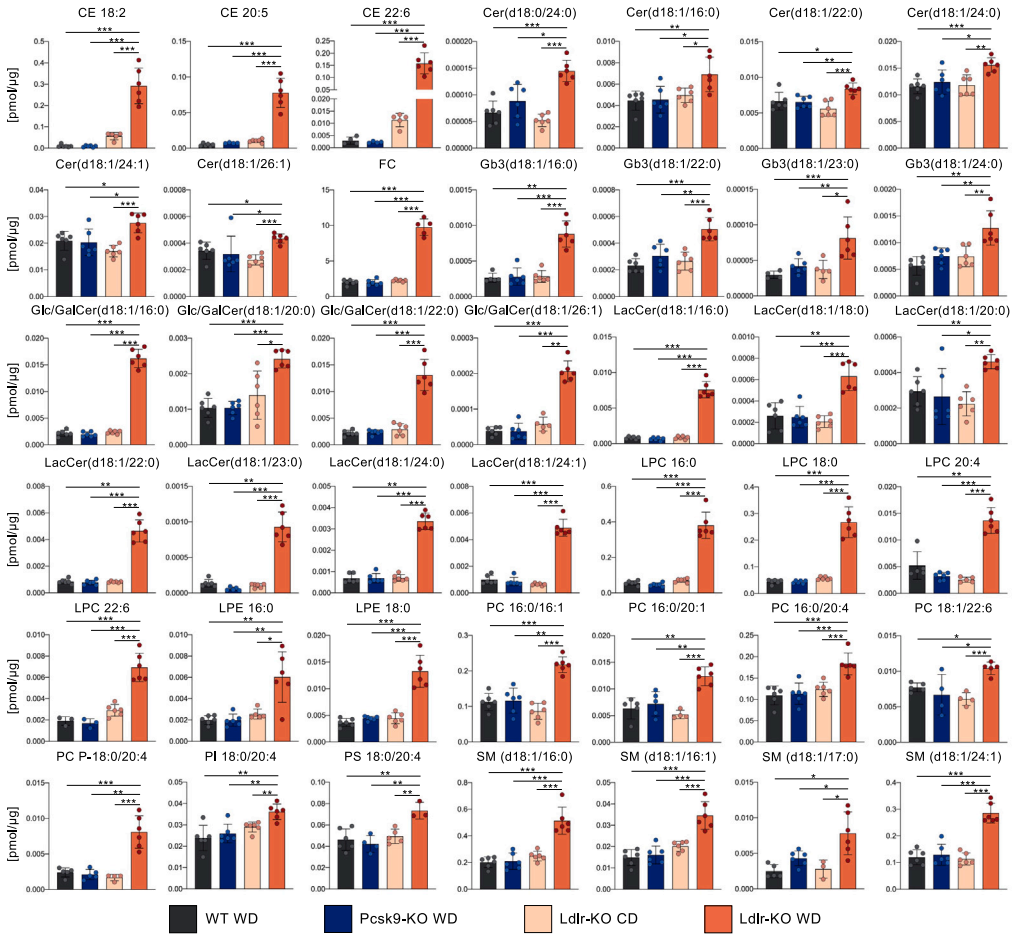

Figure 10. Absolute concentrations of the lipid species increased in the aorta of WD-fed Ldlr-KO mice compared with WD-fed WT and Pcsk9-KO mice and with CD-fed Ldlr-KO mice

Forty-two lipid species emerged from this analysis. Significant differences were determined by T test. *$p < 0.05$; **$p < 0.01$, ***$p < 0.001$. n = 3–6 per group.

with NAFLD .[55] In addition, low-density lipoproteins infiltrating in plaques present CE 18:2 as the most abundant polyunsaturated fatty acid.[12,56] CE 22:6 is likewise a cholesteryl ester identified in human endarterectomies compared with healthy carotid artery tissue.[12]

Gb3(d18:1/22:0) was found to be associated with hypobetalipoproteinemia, an inborn error of metabolism.[57] More recently, Gb3(d18:1/22:0) was among the most significant molecular lipid species associated with early markers of osteoporosis-atherosclerosis comorbidity.[58]

Glc/GalCer(d18:1/16:0) has been previously observed to be reduced in the plasma of both human carriers of PCSK9 loss-of-function mutations and Pcsk9-KO mice.[7] It is therefore possible that its concentration is somehow related to circulating LDL-C concentration, which is markedly increased in Ldlr-KO mice.

Four out of 16 lipid species belonged to LacCer. As mentioned above, LacCer accumulates in human atherosclerotic plaques compared with healthy vasculature.[59] In addition, LacCer enhances macrophage migration in plaques because of increased expression of adhesion molecules on endothelial cells[43,60]; at the same time, it has been shown that oxidized LDL increases LacCer synthesis in macrophages.[61] Also in the liver, LacCer accumulation is associated with the hepatic oxidative stress and activation of hepatic inflammatory pathways.[62]

Finally, higher SM plasma levels have been measured in patients with coronary artery disease. In addition, atherosclerotic coronary arteries obtained during coronary artery bypass grafting show higher SM concentration than healthy arteries.[44]

In order to give further consistency to these 16 markers, their concentrations were checked in plasma and aorta from apoE-KO mice fed CD or a high-fat diet.[21] The results showed that 13 of the 16 markers had increased concentration in both plasma and atherosclerotic aorta of apoE-KO mice that received the high-fat diet (the three Gb3 species included in the 16 markers, as well as liver data, were not available from this previous analysis) (Figure S12C).

In conclusion, the present study is an in-depth evaluation of the changes affecting the lipidomic profile of plasma, liver, and aorta, three districts critical for the development of atherosclerosis, in normocholesterolemic or dyslipidemic mice. In addition, data evaluation allowed: i) the identification of lipid species specifically associated with the presence of atherosclerotic plaques in the aorta; ii) to discover

the existence of lipids whose plasma pattern mirrors those found in the liver and aorta. Such lipids could represent future therapeutic targets or biomarkers for better stratification of patients.

Limitations of the study

The present experimental setting allowed the identification of potential lipid markers of atherosclerosis, but it cannot provide evidence of a causal role of those lipids in the onset and progression of the disease. Targeted experiments will be required to clarify this issue. Due to the complexity of the experimental protocol (three genotypes, three districts, and two diets), a unique time point was considered in the analysis of the lipidomic profile. Further experiments will be required to explore if the lipids emerging from this study as potential markers of atherosclerosis could also identify the progression of the disease, starting from an early-stage condition.

RESOURCE AVAILABILITY

Lead contact

Further information and requests for resources should be directed to and will be fulfilled by the lead contact, Marco Busnelli (marco.busnelli@unimi.it).

Materials availability

This study did not generate new unique reagents.

Data and code availability

- Data have been deposited in the EMBL-EBI BioStudies Database and are publicly available [BioStudies: S-BSST1634]. The accession number is also listed in the key resources table.
- This article does not report the original code.
- Any additional information required to reanalyze the data reported in this article is available from the lead contact upon request.

ACKNOWLEDGMENTS

This project has received funding from Fondazione Cariplo (2011-0645, G. Chiesa), the European Union's Horizon Europe research and innovation programme under Grant Agreement no. 101057724 - LiverTarget (G. Chiesa), from the European Union's Horizon 2020 research and innovation programme under the ERA-Net Cofund action no. 727565 (OCTOPUS project, G. Chiesa) and from MIUR "Progetto Eccellenza". This project was also supported by Piano Sostegno alla Ricerca (PSR) 2021 Linea 2 and PSR2022 Linea 2 from Università degli Studi di Milano (M. Busnelli).

We are in debt to Elda Desiderio Pinto, Luana Cremascoli and Roberta De Santis for administrative assistance. Dr. Alice Colombo is supported by the 37th cycle PhD program in "Scienze farmacologiche biomolecolari, sperimentali e cliniche", Università degli Studi di Milano. Dr. Elsa Franchi is supported by the 39th cycle PhD program in "Scienze farmacologiche biomolecolari, sperimentali e cliniche", Università degli Studi di Milano.

Part of this work was carried out at NOLIMITS, an advanced imaging facility established by the Università degli Studi di Milano.

AUTHOR CONTRIBUTIONS

Conceptualization: M.B., S.M., R.L., and G.C.; software: M.B., S.M., and M.L.; formal analysis: M.L., M.B., and S.M.; investigation: M.B., S.M., A.C., E.F., G.C., and R.L.; resources: G.C.; writing – original draft: M.B., G.C., and S.M.; visualization: M.B. and S.M.; supervision: R.L. and G.C.; project administration: G.C.; funding acquisition: S.M., M.B., and G.C.

DECLARATION OF INTERESTS

The authors declare no competing interests.

STAR★METHODS

Detailed methods are provided in the online version of this paper and include the following:

- KEY RESOURCES TABLE
- EXPERIMENTAL MODEL AND STUDY PARTICIPANT DETAILS
  - Animals and diets
- METHOD DETAILS
  - Plasma and tissue harvesting
  - Histology
  - Lipidomic analyses
  - Software
- QUANTIFICATION AND STATISTICAL ANALYSIS

SUPPLEMENTAL INFORMATION

Supplemental information can be found online at https://doi.org/10.1016/j.isci.2024.111051.

Received: April 19, 2024
Revised: July 31, 2024
Accepted: September 24, 2024
Published: September 26, 2024

REFERENCES

1. Mach, F., Baigent, C., Catapano, A.L., Koskinas, K.C., Casula, M., Badimon, L., Chapman, M.J., De Backer, G.G., Delgado, V., Ference, B.A., et al. (2020). 2019 ESC/EAS Guidelines for the management of dyslipidaemias: lipid modification to reduce cardiovascular risk. Eur. Heart J. *41*, 111–188. https://doi.org/10.1093/eurheartj/ehz455.
2. Ference, B.A., Ginsberg, H.N., Graham, I., Ray, K.K., Packard, C.J., Bruckert, E., Hegele, R.A., Krauss, R.M., Raal, F.J., Schunkert, H., et al. (2017). Low-density lipoproteins cause atherosclerotic cardiovascular disease. 1. Evidence from genetic, epidemiologic, and clinical studies. A consensus statement from the European Atherosclerosis Society Consensus Panel. Eur. Heart J. *38*, 2459–2472. https://doi.org/10.1093/eurheartj/ehx144.
3. Singh, S., and Bittner, V. (2015). Familial hypercholesterolemia–epidemiology, diagnosis, and screening. Curr. Atheroscler. Rep. *17*, 482. https://doi.org/10.1007/s11883-014-0482-5.
4. Cuchel, M., Bruckert, E., Ginsberg, H.N., Raal, F.J., Santos, R.D., Hegele, R.A., Kuivenhoven, J.A., Nordestgaard, B.G., Descamps, O.S., Steinhagen-Thiessen, E., et al. (2014). Homozygous familial hypercholesterolaemia: new insights and guidance for clinicians to improve detection and clinical management. A position paper from the Consensus Panel on Familial Hypercholesterolaemia of the European Atherosclerosis Society. Eur. Heart J. *35*, 2146–2157. https://doi.org/10.1093/eurheartj/ehu274.
5. Schreuder, M.M., Hamkour, S., Siegers, K.E., Holven, K.B., Johansen, A.K., van de Ree, M.A., Imholz, B., Boersma, E., Louters, L., Bogsrud, M.P., et al. (2023). LDL cholesterol targets rarely achieved in familial hypercholesterolemia patients: A sex and gender-specific analysis. Atherosclerosis *384*, 117117. https://doi.org/10.1016/j.atherosclerosis.2023.03.022.
6. Coppinger, C., Movahed, M.R., Azemawah, V., Peyton, L., Gregory, J., and Hashemzadeh, M. (2022). A Comprehensive Review of PCSK9 Inhibitors. J. Cardiovasc. Pharmacol. Ther. *27*, 10742484221100107. https://doi.org/10.1177/10742484221100107.
7. Jänis, M.T., Tarasov, K., Ta, H.X., Suoniemi, M., Ekroos, K., Hurme, R., Lehtimäki, T., Päivä, H., Kleber, M.E., März, W., et al. (2013). Beyond LDL-C lowering: distinct molecular sphingolipids are good indicators of proprotein convertase subtilisin/kexin type 9 (PCSK9) deficiency. Atherosclerosis *228*, 380–385. https://doi.org/10.1016/j.atherosclerosis.2013.03.029.
8. Huang, K., Wen, X.-Q., Ren, N., Yang, L., and Gao, B. (2021). Lipidomic profile in patients with a very high risk of atherosclerotic cardiovascular disease on PCSK9 inhibitor therapy. Rev. Cardiovasc. Med. *22*, 461–467. https://doi.org/10.31083/j.rcm2202052.
9. Hilvo, M., Simolin, H., Metso, J., Ruuth, M., Öörni, K., Jauhiainen, M., Laaksonen, R., and Baruch, A. (2018). PCSK9 inhibition alters the lipidome of plasma and lipoprotein fractions. Atherosclerosis *269*, 159–165. https://doi.org/10.1016/j.atherosclerosis.2018.01.004.
10. Gerszten, R.E., and Wang, T.J. (2008). The search for new cardiovascular biomarkers. Nature *451*, 949–952. https://doi.org/10.1038/nature06802.
11. Mayr, M. (2008). Metabolomics: ready for the prime time? Circ. Cardiovasc. Genet. *1*, 58–65. https://doi.org/10.1161/CIRCGENETICS.108.808329.
12. Stegemann, C., Drozdov, I., Shalhoub, J., Humphries, J., Ladroue, C., Didangelos, A., Baumert, M., Allen, M., Davies, A.H., Monaco, C., et al. (2011). Comparative lipidomics profiling of human atherosclerotic plaques. Circ. Cardiovasc. Genet. *4*, 232–242. https://doi.org/10.1161/CIRCGENETICS.110.959098.
13. Stegemann, C., Pechlaner, R., Willeit, P., Langley, S.R., Mangino, M., Mayr, U., Menni, C., Moayyeri, A., Santer, P., Rungger, G., et al. (2014). Lipidomics profiling and risk of cardiovascular disease in the prospective population-based Bruneck study. Circulation *129*, 1821–1831. https://doi.org/10.1161/CIRCULATIONAHA.113.002500.
14. Alshehry, Z.H., Mundra, P.A., Barlow, C.K., Mellett, N.A., Wong, G., McConville, M.J., Simes, J., Tonkin, A.M., Sullivan, D.R., Barnes, E.H., et al. (2016). Plasma Lipidomic Profiles Improve on Traditional Risk Factors for the Prediction of Cardiovascular Events in Type 2 Diabetes Mellitus. Circulation *134*, 1637–1650. https://doi.org/10.1161/CIRCULATIONAHA.116.023233.
15. Mundra, P.A., Barlow, C.K., Nestel, P.J., Barnes, E.H., Kirby, A., Thompson, P., Sullivan, D.R., Alshehry, Z.H., Mellett, N.A., Huynh, K., et al. (2018). Large-scale plasma lipidomic profiling identifies lipids that predict cardiovascular events in secondary prevention. JCI Insight *3*, e121326. https://doi.org/10.1172/jci.insight.121326.
16. Kauhanen, D., Sysi-Aho, M., Koistinen, K.M., Laaksonen, R., Sinisalo, J., and Ekroos, K. (2016). Development and validation of a high-throughput LC-MS/MS assay for routine measurement of molecular ceramides. Anal. Bioanal. Chem. *408*, 3475–3483. https://doi.org/10.1007/s00216-016-9425-z.
17. Hilvo, M., Meikle, P.J., Pedersen, E.R., Tell, G.S., Dhar, I., Brenner, H., Schöttker, B., Lääperi, M., Kauhanen, D., Koistinen, K.M., et al. (2020). Development and validation of a ceramide- and phospholipid-based cardiovascular risk estimation score for coronary artery disease patients. Eur. Heart J. *41*, 371–380. https://doi.org/10.1093/eurheartj/ehz387.
18. Slijkhuis, N., Razzi, F., Korteland, S.-A., Heijs, B., van Gaalen, K., Duncker, D.J., van der Steen, A.F.W., van Steijn, V., van Beusekom, H.M.M., and van Soest, G. (2024). Spatial lipidomics of coronary atherosclerotic plaque development in a familial hypercholesterolemia swine model. J. Lipid Res. *65*, 100504. https://doi.org/10.1016/j.jlr.2024.100504.
19. Chen, Y., Wen, S., Jiang, M., Zhu, Y., Ding, L., Shi, H., Dong, P., Yang, J., and Yang, Y. (2017). Atherosclerotic dyslipidemia revealed by plasma lipidomics on ApoE-/- mice fed a high-fat diet. Atherosclerosis *262*, 78–86. https://doi.org/10.1016/j.atherosclerosis.2017.05.010.
20. Cao, J., Goossens, P., Martin-Lorenzo, M., Dewez, F., Claes, B.S.R., Biessen, E.A.L., Heeren, R.M.A., and Balluff, B. (2020). Atheroma-Specific Lipids in ldlr-/- and apoe-/- Mice Using 2D and 3D Matrix-Assisted Laser Desorption/Ionization Mass Spectrometry Imaging. J. Am. Soc. Mass Spectrom. *31*, 1825–1832. https://doi.org/10.1021/jasms.0c00070.
21. Busnelli, M., Manzini, S., Colombo, A., Franchi, E., Lääperi, M., Laaksonen, R., and Chiesa, G. (2023). Effect of Diets on Plasma and Aorta Lipidome: A Study in the apoE Knockout Mouse Model. Mol. Nutr. Food Res. *67*, e2200367. https://doi.org/10.1002/mnfr.202200367.
22. Vik, R., Busnelli, M., Parolini, C., Bjørndal, B., Holm, S., Bohov, P., Halvorsen, B., Brattelid, T., Manzini, S., Ganzetti, G.S., et al. (2013). An immunomodulating fatty acid analogue targeting mitochondria exerts anti-atherosclerotic effect beyond plasma cholesterol-lowering activity in apoe(-/-) mice. PLoS One *8*, e81963. https://doi.org/10.1371/journal.pone.0081963.
23. Karagiannides, I., Abdou, R., Tzortzopoulou, A., Voshol, P.J., and Kypreos, K.E. (2008). Apolipoprotein E predisposes to obesity and related metabolic dysfunctions in mice. FEBS J. *275*, 4796–4809. https://doi.org/10.1111/j.1742-4658.2008.06619.x.
24. Ngai, Y.F., Quong, W.L., Glier, M.B., Glavas, M.M., Babich, S.L., Innis, S.M., Kieffer, T.J., and Gibson, W.T. (2010). Ldlr-/- mice display decreased susceptibility to Western-type diet-induced obesity due to increased thermogenesis. Endocrinology *151*, 5226–5236. https://doi.org/10.1210/en.2010-0496.
25. Tolleshaug, H., Hobgood, K.K., Brown, M.S., and Goldstein, J.L. (1983). The LDL receptor locus in familial hypercholesterolemia: multiple mutations disrupt transport and processing of a membrane receptor. Cell *32*, 941–951. https://doi.org/10.1016/0092-8674(83)90079-x.
26. Kent, S.T., Rosenson, R.S., Avery, C.L., Chen, Y.-D.I., Correa, A., Cummings, S.R., Cupples, L.A., Cushman, M., Evans, D.S., Gudnason, V., et al. (2017). PCSK9 Loss-of-Function Variants, Low-Density Lipoprotein Cholesterol, and Risk of Coronary Heart Disease and Stroke: Data From 9 Studies of Blacks and Whites. Circ. Cardiovasc. Genet. *10*, e001632. https://doi.org/10.1161/CIRCGENETICS.116.001632.
27. Garcia, C., Andersen, C.J., and Blesso, C.N. (2023). The Role of Lipids in the Regulation of Immune Responses. Nutrients *15*, 3899. https://doi.org/10.3390/nu15183899.
28. Radzikowska, U., Rinaldi, A.O., Çelebi Sözener, Z., Karaguzel, D., Wojcik, M., Cypryk, K., Akdis, M., Akdis, C.A., and Sokolowska, M. (2019). The Influence of Dietary Fatty Acids on Immune Responses. Nutrients *11*, 2990. https://doi.org/10.3390/nu11122990.
29. Wang, S., Wu, D., Lamon-Fava, S., Matthan, N.R., Honda, K.L., and Lichtenstein, A.H. (2009). In vitro fatty acid enrichment of macrophages alters inflammatory response and net cholesterol accumulation. Br. J. Nutr. *102*, 497–501. https://doi.org/10.1017/S0007114509231758.
30. Tam, T.H., Chan, K.L., Boroumand, P., Liu, Z., Brozinick, J.T., Bui, H.H., Roth, K., Wakefield, C.B., Penuela, S., Bilan, P.J., and Klip, A. (2020). Nucleotides released from palmitate-activated murine macrophages attract neutrophils. J. Biol. Chem. *295*, 4902–4911. https://doi.org/10.1074/jbc.RA119.010868.
31. Qin, C., Nagao, T., Grosheva, I., Maxfield, F.R., and Pierini, L.M. (2006). Elevated plasma membrane cholesterol content alters macrophage signaling and function. Arterioscler. Thromb. Vasc. Biol. *26*, 372–378.

https://doi.org/10.1161/01.ATV.0000197848.67999.e1.
32. Pagler, T.A., Wang, M., Mondal, M., Murphy, A.J., Westerterp, M., Moore, K.J., Maxfield, F.R., and Tall, A.R. (2011). Deletion of ABCA1 and ABCG1 impairs macrophage migration because of increased Rac1 signaling. Circ. Res. *108*, 194–200. https://doi.org/10.1161/CIRCRESAHA.110.228619.
33. Yang, W., Bai, Y., Xiong, Y., Zhang, J., Chen, S., Zheng, X., Meng, X., Li, L., Wang, J., Xu, C., et al. (2016). Potentiating the antitumour response of CD8(+) T cells by modulating cholesterol metabolism. Nature *531*, 651–655. https://doi.org/10.1038/nature17412.
34. Nordestgaard, B.G. (2016). Triglyceride-Rich Lipoproteins and Atherosclerotic Cardiovascular Disease: New Insights From Epidemiology, Genetics, and Biology. Circ. Res. *118*, 547–563. https://doi.org/10.1161/CIRCRESAHA.115.306249.
35. Maxfield, F.R., Steinfeld, N., and Ma, C.-I.J. (2023). The formation and consequences of cholesterol-rich deposits in atherosclerotic lesions. Front. Cardiovasc. Med. *10*, 1148304. https://doi.org/10.3389/fcvm.2023.1148304.
36. Albeituni, S., and Stiban, J. (2019). Roles of Ceramides and Other Sphingolipids in Immune Cell Function and Inflammation. Adv. Exp. Med. Biol. *1161*, 169–191. https://doi.org/10.1007/978-3-030-21735-8_15.
37. Chiricozzi, E., Loberto, N., Schiumarini, D., Samarani, M., Mancini, G., Tamanini, A., Lippi, G., Dechecchi, M.C., Bassi, R., Giussani, P., and Aureli, M. (2018). Sphingolipids role in the regulation of inflammatory response: From leukocyte biology to bacterial infection. J. Leukoc. Biol. *103*, 445–456. https://doi.org/10.1002/JLB.3MR0717-269R.
38. Lee, M., Lee, S.Y., and Bae, Y.-S. (2023). Functional roles of sphingolipids in immunity and their implication in disease. Exp. Mol. Med. *55*, 1110–1130. https://doi.org/10.1038/s12276-023-01018-9.
39. Adam, D., Heinrich, M., Kabelitz, D., and Schütze, S. (2002). Ceramide: does it matter for T cells? Trends Immunol. *23*, 1–4. https://doi.org/10.1016/s1471-4906(01)02091-9.
40. Schissel, S.L., Tweedie-Hardman, J., Rapp, J.H., Graham, G., Williams, K.J., and Tabas, I. (1996). Rabbit aorta and human atherosclerotic lesions hydrolyze the sphingomyelin of retained low-density lipoprotein. Proposed role for arterial-wall sphingomyelinase in subendothelial retention and aggregation of atherogenic lipoproteins. J. Clin. Invest. *98*, 1455–1464. https://doi.org/10.1172/JCI118934.
41. Laaksonen, R., Ekroos, K., Sysi-Aho, M., Hilvo, M., Vihervaara, T., Kauhanen, D., Suoniemi, M., Hurme, R., März, W., Scharnagl, H., et al. (2016). Plasma ceramides predict cardiovascular death in patients with stable coronary artery disease and acute coronary syndromes beyond LDL-cholesterol. Eur. Heart J. *37*, 1967–1976. https://doi.org/10.1093/eurheartj/ehw148.
42. Smith, E.B. (1960). Intimal and medial lipids in human aortas. Lancet (London, England) *1*, 799–803. https://doi.org/10.1016/s0140-6736(60)90680-2.
43. Edsfeldt, A., Dunér, P., Ståhlman, M., Mollet, I.G., Asciutto, G., Grufman, H., Nitulescu, M., Persson, A.F., Fisher, R.M., Melander, O., et al. (2016). Sphingolipids Contribute to Human Atherosclerotic Plaque Inflammation. Arterioscler. Thromb. Vasc. Biol. *36*, 1132–1140. https://doi.org/10.1161/ATVBAHA.116.305675.
44. Yu, Z., Peng, Q., and Huang, Y. (2019). Potential therapeutic targets for atherosclerosis in sphingolipid metabolism. Clin. Sci. *133*, 763–776. https://doi.org/10.1042/CS20180911.
45. Zarate, Y.A., and Hopkin, R.J. (2008). Fabry's disease. Lancet (London, England) *372*, 1427–1435. https://doi.org/10.1016/S0140-6736(08)61589-5.
46. Choi, S., Kim, J.A., Na, H.-Y., Cho, S.-E., Park, S., Jung, S.-C., and Suh, S.H. (2014). Globotriaosylceramide induces lysosomal degradation of endothelial KCa3.1 in fabry disease. Arterioscler. Thromb. Vasc. Biol. *34*, 81–89. https://doi.org/10.1161/ATVBAHA.113.302200.
47. Schmitz, G., and Ruebsaamen, K. (2010). Metabolism and atherogenic disease association of lysophosphatidylcholine. Atherosclerosis *208*, 10–18. https://doi.org/10.1016/j.atherosclerosis.2009.05.029.
48. Tan, S.H., Koh, H.W.L., Chua, J.Y., Burla, B., Ong, C.C., Teo, L.S.L., Yang, X., Benke, P.I., Choi, H., Torta, F., et al. (2022). Variability of the Plasma Lipidome and Subclinical Coronary Atherosclerosis. Arterioscler. Thromb. Vasc. Biol. *42*, 100–112. https://doi.org/10.1161/ATVBAHA.121.316847.
49. Aiyar, N., Disa, J., Ao, Z., Ju, H., Nerurkar, S., Willette, R.N., Macphee, C.H., Johns, D.G., and Douglas, S.A. (2007). Lysophosphatidylcholine induces inflammatory activation of human coronary artery smooth muscle cells. Mol. Cell. Biochem. *295*, 113–120. https://doi.org/10.1007/s11010-006-9280-x.
50. Oka, H., Kugiyama, K., Doi, H., Matsumura, T., Shibata, H., Miles, L.A., Sugiyama, S., and Yasue, H. (2000). Lysophosphatidylcholine induces urokinase-type plasminogen activator and its receptor in human macrophages partly through redox-sensitive pathway. Arterioscler. Thromb. Vasc. Biol. *20*, 244–250. https://doi.org/10.1161/01.atv.20.1.244.
51. Ryborg, A.K., Deleuran, B., Thestrup-Pedersen, K., and Kragballe, K. (1994). Lysophosphatidylcholine: a chemoattractant to human T lymphocytes. Arch. Dermatol. Res. *286*, 462–465. https://doi.org/10.1007/BF00371572.
52. Weber, C., Erl, W., and Weber, P.C. (1995). Enhancement of monocyte adhesion to endothelial cells by oxidatively modified low-density lipoprotein is mediated by activation of CD11b. Biochem. Biophys. Res. Commun. *206*, 621–628. https://doi.org/10.1006/bbrc.1995.1088.
53. Nakano, T., Raines, E.W., Abraham, J.A., Klagsbrun, M., and Ross, R. (1994). Lysophosphatidylcholine upregulates the level of heparin-binding epidermal growth factor-like growth factor mRNA in human monocytes. Proc. Natl. Acad. Sci. USA *91*, 1069–1073. https://doi.org/10.1073/pnas.91.3.1069.
54. Nishi, E., Kume, N., Ochi, H., Moriwaki, H., Wakatsuki, Y., Higashiyama, S., Taniguchi, N., and Kita, T. (1997). Lysophosphatidylcholine increases expression of heparin-binding epidermal growth factor-like growth factor in human T lymphocytes. Circ. Res. *80*, 638–644. https://doi.org/10.1161/01.res.80.5.638.
55. Vvedenskaya, O., Rose, T.D., Knittelfelder, O., Palladini, A., Wodke, J.A.H., Schuhmann, K., Ackerman, J.M., Wang, Y., Has, C., Brosch, M., et al. (2021). Nonalcoholic fatty liver disease stratification by liver lipidomics. J. Lipid Res. *62*, 100104. https://doi.org/10.1016/j.jlr.2021.100104.
56. Slijkhuis, N., Towers, M., Mirzaian, M., Korteland, S.-A., Heijs, B., van Gaalen, K., Nieuwenhuizen, I., Nigg, A., van der Heiden, K., de Rijke, Y.B., et al. (2023). Identifying lipid traces of atherogenic mechanisms in human carotid plaque. Atherosclerosis *385*, 117340. https://doi.org/10.1016/j.atherosclerosis.2023.117340.
57. Dawson, G., Kruski, A.W., and Scanu, A.M. (1976). Distribution of glycosphingolipids in the serum lipoproteins of normal human subjects and patients with hypo- and hyperlipidemias. J. Lipid Res. *17*, 125–131.
58. Mishra, B.H., Mishra, P.P., Mononen, N., Hilvo, M., Sievänen, H., Juonala, M., Laaksonen, M., Hutri-Kähönen, N., Viikari, J., Kähönen, M., et al. (2021). Uncovering the shared lipidomic markers of subclinical osteoporosis-atherosclerosis comorbidity: The Young Finns Study. Bone *151*, 116030. https://doi.org/10.1016/j.bone.2021.116030.
59. Mukhin, D.N., Chao, F.F., and Kruth, H.S. (1995). Glycosphingolipid accumulation in the aortic wall is another feature of human atherosclerosis. Arterioscler. Thromb. Vasc. Biol. *15*, 1607–1615. https://doi.org/10.1161/01.atv.15.10.1607.
60. Gong, N., Wei, H., Chowdhury, S.H., and Chatterjee, S. (2004). Lactosylceramide recruits PKCalpha/epsilon and phospholipase A2 to stimulate PECAM-1 expression in human monocytes and adhesion to endothelial cells. Proc. Natl. Acad. Sci. USA *101*, 6490–6495. https://doi.org/10.1073/pnas.0308684101.
61. Grandl, M., Bared, S.M., Liebisch, G., Werner, T., Barlage, S., and Schmitz, G. (2006). E-LDL and Ox-LDL differentially regulate ceramide and cholesterol raft microdomains in human Macrophages. Cytometry A. *69*, 189–191. https://doi.org/10.1002/cyto.a.20232.
62. Apostolopoulou, M., Gordillo, R., Koliaki, C., Gancheva, S., Jelenik, T., De Filippo, E., Herder, C., Markgraf, D., Jankowiak, F., Esposito, I., et al. (2018). Specific Hepatic Sphingolipids Relate to Insulin Resistance, Oxidative Stress, and Inflammation in Nonalcoholic Steatohepatitis. Diabetes Care *41*, 1235–1243. https://doi.org/10.2337/dc17-1318.
63. van der Walt, S., Colbert, S.C., and Varoquaux, G. (2011). The NumPy Array: A Structure for Efficient Numerical Computation. Comput. Sci. Eng. *13*, 22–30. https://doi.org/10.1109/MCSE.2011.37.
64. McKinney, W. (2010). Data Structures for Statistical Computing in Python. In Proceedings of the 9th Python in Science Conference, S. van der Walt and J. Millman, eds., pp. 56–61. https://doi.org/10.25080/Majora-92bf1922-00a.
65. Hunter, J.D. (2007). Matplotlib: A 2D Graphics Environment. Comput. Sci. Eng. *9*, 90–95. https://doi.org/10.1109/MCSE.2007.55.
66. Waskom, M. (2021). seaborn: statistical data visualization. J. Open Source Softw. *6*, 3021. https://doi.org/10.21105/joss.03021.
67. Pedregosa, F., Varoquaux, G., Gramfort, A., Michel, V., Thirion, B., Grisel, O., Blondel, M., Prettenhofer, P., Weiss, R., Dubourg, V., et al. (2011). Scikit-learn: Machine Learning in {P}ython. J. Mach. Learn. Res. *12*, 2825–2830.
68. Manzini, S., Busnelli, M., Colombo, A., Kiamehr, M., and Chiesa, G. (2020). liputils: a Python module to manage individual fatty acid moieties from complex lipids. Sci. Rep.

10, 13368. https://doi.org/10.1038/s41598-020-70259-9.

69. Busnelli, M., Manzini, S., Colombo, A., Franchi, E., Chiara, M., Zaffaroni, G., Horner, D., and Chiesa, G. (2023). Effect of diet and genotype on the miRNome of mice with altered lipoprotein metabolism. iScience *26*, 107615. https://doi.org/10.1016/j.isci.2023.107615.
70. Arnaboldi, F., Busnelli, M., Cornaghi, L., Manzini, S., Parolini, C., Dellera, F., Ganzetti, G.S., Sirtori, C.R., Donetti, E., and Chiesa, G. (2015). High-density lipoprotein deficiency in genetically modified mice deeply affects skin morphology: A structural and ultrastructural study. Exp. Cell Res. *338*, 105–112. https://doi.org/10.1016/j.yexcr.2015.07.032.
71. Manzini, S., Busnelli, M., Parolini, C., Minoli, L., Ossoli, A., Brambilla, E., Simonelli, S., Lekka, E., Persidis, A., Scanziani, E., and Chiesa, G. (2019). Topiramate protects apoE-deficient mice from kidney damage without affecting plasma lipids. Pharmacol. Res. *141*, 189–200. https://doi.org/10.1016/j.phrs.2018.12.022.
72. Busnelli, M., Manzini, S., Chiara, M., Colombo, A., Fontana, F., Oleari, R., Potì, F., Horner, D., Bellosta, S., and Chiesa, G. (2021). Aortic Gene Expression Profiles Show How ApoA-I Levels Modulate Inflammation, Lysosomal Activity, and Sphingolipid Metabolism in Murine Atherosclerosis. Arterioscler. Thromb. Vasc. Biol. *41*, 651–667. https://doi.org/10.1161/ATVBAHA.120.315669.
73. Busnelli, M., Manzini, S., Colombo, A., Franchi, E., Bonacina, F., Chiara, M., Arnaboldi, F., Donetti, E., Ambrogi, F., Oleari, R., et al. (2022). Lack of ApoA-I in ApoEKO Mice Causes Skin Xanthomas, Worsening of Inflammation, and Increased Coronary Atherosclerosis in the Absence of Hyperlipidemia. Arterioscler. Thromb. Vasc. Biol. *42*, 839–856. https://doi.org/10.1161/ATVBAHA.122.317790.
74. Busnelli, M., Manzini, S., Bonacina, F., Soldati, S., Barbieri, S.S., Amadio, P., Sandrini, L., Arnaboldi, F., Donetti, E., Laaksonen, R., et al. (2020). Fenretinide treatment accelerates atherosclerosis development in apoE-deficient mice in spite of beneficial metabolic effects. Br. J. Pharmacol. *177*, 328–345. https://doi.org/10.1111/bph.14869.
75. Jung, H.R., Sylvänne, T., Koistinen, K.M., Tarasov, K., Kauhanen, D., and Ekroos, K. (2011). High throughput quantitative molecular lipidomics. Biochim. Biophys. Acta *1811*, 925–934. https://doi.org/10.1016/j.bbalip.2011.06.025.
76. Busnelli, M., Manzini, S., Hilvo, M., Parolini, C., Ganzetti, G.S., Dellera, F., Ekroos, K., Jänis, M., Escalante-Alcalde, D., Sirtori, C.R., et al. (2017). Liver-specific deletion of the Plpp3 gene alters plasma lipid composition and worsens atherosclerosis in apoE$^{-/-}$ mice. Sci. Rep. *7*, 44503. https://doi.org/10.1038/srep44503.
77. Ståhlman, M., Ejsing, C.S., Tarasov, K., Perman, J., Borén, J., and Ekroos, K. (2009). High-throughput shotgun lipidomics by quadrupole time-of-flight mass spectrometry. J. Chromatogr., B: Anal. Technol. Biomed. Life Sci. *877*, 2664–2672. https://doi.org/10.1016/j.jchromb.2009.02.037.
78. Ekroos, K., Ejsing, C.S., Bahr, U., Karas, M., Simons, K., and Shevchenko, A. (2003). Charting molecular composition of phosphatidylcholines by fatty acid scanning and ion trap MS3 fragmentation. J. Lipid Res. *44*, 2181–2192. https://doi.org/10.1194/jlr.D300020-JLR200.

STAR★METHODS

KEY RESOURCES TABLE

REAGENT or RESOURCE	SOURCE	IDENTIFIER
Chemicals, peptides, and recombinant proteins		
Diet: Standard rodent chow	Mucedola	4RF21
Diet: Western-type	Envigo	TD.88137
Isoflurane	Merial	N01AB06
Tissue-Tek O.C.T. Compound	Sakura Finetek	4583
Hematoxylin	Bio-Optica	05-06002
Eosin	Bio-Optica	05-10003
Oil Red O	Bio-Optica	04-220923
Deposited data		
Lipid quantification data (produced by this study)	EMBL-EBI Biostudies Database	BioStudies: S- BSST1634 - https://doi.org/10.6019/S-BSST1634
Experimental models: Organisms/strains		
Mouse: C57BL6/J	JAX/Charles River Laboratories	Strain: 000664; RRID: IMSR_JAX:000664
Mouse: Ldlr-KO	JAX/Charles River Laboratories	Strain: 002207; RRID: IMSR_JAX:002207
Mouse: Pcsk9-KO	JAX/Charles River Laboratories	Strain: 005993; RRID: IMSR_JAX:005993
Software and algorithms		
numpy	(van der Walt et al.[63])	https://numpy.org/
pandas	(McKinney et al.[64])	https://pandas.pydata.org/
matplotlib	(Hunter et al.[65])	https://bioconductor.org/packages/release/bioc/html/DESeq2.html
seaborn	Waskom et al.[66])	https://seaborn.pydata.org/
scikit-learn	(Pedregosa et al.[67])	https://scikit-learn.org/
liputils	(Manzini et al.[68])	https://github.com/Stemanz/liputils
Prism 9	GraphPad	https://www.graphpad.com/
Tableau	Salesforce	https://www.tableau.com/
NDP.view2	Hamamatsu Photonics	https://www.hamamatsu.com/jp/en/

EXPERIMENTAL MODEL AND STUDY PARTICIPANT DETAILS

Animals and diets

Procedures involving animals and their care were conducted in accordance with institutional guidelines that are in compliance with national (D.L. No. 26, March 4, 2014, G.U. No. 61 March 14, 2014) and international laws and policies (EEC Council Directive 2010/63, September 22, 2010: Guide for the Care and Use of Laboratory Animals, United States National Research Council, 2011). The experimental protocol was approved by the Italian Ministry of Health (Protocollo n° 04/2012).

C57BL/6J controls (WT; RRID:IMSR_JAX:000664), homozygous Low-Density Lipoprotein receptor gene knock-out (Ldlr-KO; RRID:IMSR_JAX:002207) and homozygous Proprotein convertase subtilisin/kexin 9 gene knock-out (Pcsk9-KO; RRID:IMSR_JAX:005993) mice in the C57BL/6 background were purchased from Charles River Laboratories (Calco, Italy).[69] Mice were randomized into experimental groups (randomly allocated into groups, by weight, until there was no statistical significance among groups), housed 3 per cage and kept under standard laboratory conditions (12 hours light cycle, temperature 22±1°C, humidity 55±5%). From the sixth week from birth, mice were fed for 16 weeks either standard chow diet (CD), containing 3.0% soybean oil (4RF21, Mucedola, Settimo Milanese, Italy), or Western-type diet (WD), containing 21.0% milkfat, 34% sucrose and 0.2% cholesterol (TD.88137, Envigo, Bresso, Italy). The fatty acid composition of the two diets is shown in Table 1. With the aim of identifying a gender-independent lipidomic signature, each experimental group was composed of 6 mice (3 males, 3 females).

METHOD DETAILS

Plasma and tissue harvesting

At the end of the experimental period, blood was collected from the retro-orbital plexus into a capillary tube under general anesthesia with 2% isoflurane into tubes containing 0.1% w/v EDTA, and plasma was separated after centrifugation for 8 minutes at 10,000×g at 4°C[70] Mice were sacrificed under general anaesthesia with 2% isoflurane and the blood was removed by perfusion with PBS. Hearts were removed, fixed for 24h in 10% formalin, then transferred in 30% sucrose in 1× PBS for 24h, and embedded in OCT.[71] The aorta was rapidly harvested and cleaned,[72] immediately snap-frozen in liquid nitrogen and stored at −80°C until lipidomic analyses. Likewise, the liver was weighed and snap-frozen in liquid nitrogen for subsequent analyses.

Histology

Serial cryosections (7 μm thick) of the aortic sinus were cut and stained with hematoxylin and eosin (H&E) to detect plaque area.[73,74] Sections (7 μm thick) obtained from snap-frozen liver portions embedded in O.C.T. were stained with Oil Red O to detect neutral lipid deposition (04-220923, Bio-Optica, Italy). Digitized scans obtained with the Nanozoomer S60 were subsequently processed with the NDP.view2 software (Hamamatsu Photonics, Japan) and evaluated by two blinded operators.

Lipidomic analyses

A total of 21 lipid classes were analyzed in mouse organs/tissues: CE, Cer d18:0, Cer d18:1, DAG, FC, Gb3, Glc/GalCer, LacCer, LPC, LPE, LPI, PA, PC, PC O/PC P, PE, PE O/PE P, PG, PI, PS, SM, TAG.

The tissue samples were pulverized with CP02 CryoPrep Dry Pulverization System (Covaris) and resuspended in ice-cold methanol containing 0.1% butyl-hydroxy-toluene (BHT) in a concentration of 100 mg/ml. Lipids were extracted using a modified Folch lipid extraction[75] performed on a Hamilton Microlab Star robot. Samples were spiked with known amounts of non-endogeneous synthetic internal standards. After lipid extraction, samples were reconstituted in chloroform:methanol (1:2, v/v) and a synthetic external standard was post-extract spiked to the extracts.[76] The extracts were stored at -20°C prior to MS analysis. The lipid extracts were analyzed on a hybrid triple quadrupole/linear ion trap mass spectrometer (QTRAP 5500) equipped with a robotic nanoflow ion source (NanoMate HD) according to Ståhlman and colleagues.[77] Molecular lipids were analyzed in both positive and negative ion modes using multiple precursor ion scanning (MPIS) and neutral loss (NL) based methods.[21,78] TAG were analysed in positive ion mode. For quantification of free cholesterol, an aliquot of each lipid extract was treated with acetyl chloride to derivatize free cholesterol to modified cholesteryl ester species. Ceramides were analyzed on a 5500 QTRAP equipped with an ultra-high pressure liquid chromatography (UHPLC) system (CTC HTC PAL autosampler and Rheos Allegro pump) using in-house developed multiple reaction monitoring (MRM) –based methods in positive or negative ion modes. The lipids were normalized to their respective internal standard and to sample amounts. Plasma lipidomic data are provided as pmol μL^{-1}, whereas those from aorta and liver were expressed as pmol μg^{-1} of tissue. Data has been deposited in the EMBL-EBI Biostudies Database with accession number S-BSST1634.

Software

Data was processed with numpy (version 1.19.5),[63] and pandas (version 1.2.1)[64]; data visualization was performed with matplotlib (version 3.3.4),[65] and seaborn (version 0.11.1)[66] libraries for the Python programming language. Principal Component Analysis (PCA) was performed with Scikit-learn (version 0.24.1).[67] Individual fatty acid residues were extracted from the lipidomic dataset with liputils (version 0.16.2).[68] Lipidomic data were charted using Tableau (Tableau Software, version 10.3) and GraphPad Prism version 9. Lipid Maps reaction explorer (https://www.lipidmaps.org/resources/tools/reactions) was used to visualize lipid pathways.

QUANTIFICATION AND STATISTICAL ANALYSIS

Data on body weight, liver weight, lipid classes, atherosclerosis at the aortic sinus are expressed as mean ± SD. After testing for normal distribution, same-diet (different genotypes) comparisons were performed by ANOVA, followed by Tukey post-hoc; otherwise, same-genotype (different diet) comparisons were tested for statistical significance with Student's T-test (two-tailed). Lipid species are expressed as median values and tested for statistical significance using Student's T-test (two-tailed). GraphPad Prism Version 9 was used. In charts: *$p < 0.05$, **$p < 0.01$, ***$p < 0.001$, ****$p < 0.0001$.